frontiers | Frontiers in Earth Science

TYPE Review
PUBLISHED 09 May 2023
DOI 10.3389/feart.2023.1160285

OPEN ACCESS

EDITED BY
Steven L. Forman,
Baylor University, United States

REVIEWED BY
Peiyun Cong,
Yunnan University, China
Elizabeth Petsios,
Baylor University, United States
James Lamsdell,
West Virginia University, United States

*CORRESPONDENCE
Gaëtan J.-M. Potin,
gaetan.jm.potin@outlook.fr
Allison C. Daley,
allison.daley@unil.ch

RECEIVED 07 February 2023
ACCEPTED 18 April 2023
PUBLISHED 09 May 2023

CITATION
Potin GJ-M and Daley AC (2023), The significance of *Anomalocaris* and other Radiodonta for understanding paleoecology and evolution during the Cambrian explosion.
Front. Earth Sci. 11:1160285.
doi: 10.3389/feart.2023.1160285

The significance of *Anomalocaris* and other Radiodonta for understanding paleoecology and evolution during the Cambrian explosion

Gaëtan J.-M. Potin* and Allison C. Daley*

Institute of Earth Sciences, University of Lausanne, Lausanne, Switzerland

One of the most widespread and diverse animal groups of the Cambrian Explosion is a clade of stem lineage arthropods known as Radiodonta, which lived exclusively in the early Paleozoic. First reported in 1892 with *Anomalocaris canadensis*, radiodonts are now one of the best known early animal groups with excellent representation in the fossil record, and are ubiquitous components of *Konservat-Lagerstätten* from the Cambrian and the Early Ordovician. These large swimmers were characterised by a segmented body bearing laterally-oriented flaps, and a head with a distinct radial oral cone, a pair of large frontal appendages adapted for different feeding modes, compound eyes on stalks, and prominent head carapaces. Radiodonts inform on the paleoecology of early animal communities and the steps involved in euarthropod evolution. Four families within Radiodonta have been established. The raptorial predator families Anomalocarididae and Amplectobeluidae were dominant early in the evolutionary history of Radiodonta, but were later overtaken by the mega-diverse and widespread Hurdiidae, which has a more generalised sediment-sifting predatory mode. Suspension feeding, notably in the families Tamisiocarididae and Hurdiidae, also evolved at least twice in the history of the clade. The well-preserved anatomical features of the radiodont body and head have also provided insights into the evolution of characteristic features of Euarthropoda, such as the biramous limbs, compound eyes, and organisation of the head. With 37 species recovered from all major paleocontinents of the Cambrian and Early Ordovician, Radiodonta provides a unique opportunity for revealing evolutionary patterns during the Cambrian Explosion.

KEYWORDS

Arthropoda, Radiodonta, *Anomalocaris*, Cambrian, fossils, lagerstätten, review

1 Introduction

The Cambrian Explosion, followed by the Great Ordovician Biodiversification Event (GOBE) are two of the most important events in the history of life (Paterson et al., 2019; Budd, 2021; Saleh et al., 2022a). Those events saw the rapid emergence and diversification of nearly all animal phyla, and the building of functioning complex modern ecosystems. During the Cambrian Explosion the most successful animal phylum, Arthropoda, appeared and rapidly evolved into a highly diverse and

abundant component of early animal communities (Daley et al., 2018; Edgecombe, 2020; Budd, 2021). Arthropods represent 85% of living animals and they were also dominant in the fossil record during the last 500 million years, including many diverse groups such as trilobites, decapods and ostracods (Edgecombe, 2020). The Cambrian Explosion, and the early evolution of Arthropoda are both well documented by exceptionally preserved fossils sites called Burgess-Shale type *Lagerstätten* (Conway Morris, 1985; Holmes et al., 2018). These *Lagerstätten* provide a relatively complete view of the earliest animal ecosystems and how they were structured.

The most emblematic fossil group from the Cambrian Explosion is Radiodonta, best represented by *Anomalocaris canadensis* (Figure 1C), a giant apex predator of the famous Burgess Shale (Daley and Edgecombe, 2014). Radiodonts, informally called anomalocaridids, are an extinct order of nektonic predators that lived from Cambrian Series 2 Stage 3 to the Early Ordovician, and possibly into the Lower Devonian with the enigmatic *Schinderhannes* (Kühl et al., 2009; Daley and Legg, 2015; Van Roy et al., 2015; Edgecombe, 2020). A total of 37 species have been placed in or associated with Radiodonta, and all are predators, even though the predation strategy differs between taxa (Daley and Budd, 2010; Daley et al., 2013a; Daley and Edgecombe, 2014; Van Roy et al., 2015; Moysiuk and Caron, 2021). Radiodonts all have a segmented body with laterally-oriented flaps and setal blades, and a head characterised by a pair of large compound eyes on stalks, a pair of large, segmented frontal appendages, cephalic carapaces, and radially arranged plates surrounding the mouth (Figure 2). This last feature, the oral cone (Figure 3), gives rise to the name of the order Radiodonta (Collins, 1996), although it is now known that some radiodonts do not possess a circular oral cone structure (Cong et al., 2017; Cong et al., 2018).

Anomalocaris canadensis (Figure 1C) was the first radiodont described in the literature by Whiteaves (1892) but it was then interpreted as a crustacean, and isolated specimens of sclerotised body parts including the oral cone (Figure 3), frontal appendages (Figures 4, 5), and cephalic carapaces (Figures 6C–E) were also described as separate genera and species. It was not until the pivotal work of Whittington and Briggs (1985) that the first description of a complete radiodont body was realized. This complex history of description is reviewed in detail by Collins (1996), with later discoveries in Daley et al. (2009) and Daley and Bergström (2012) (see Supplementary Table S1 for historical names of body parts and their current terminology). Collins (1996) erected the order Radiodonta after describing new whole body Burgess Shale specimens. During the 1980s and 1990s, isolated appendages and oral cones were reported from a handful of localities in the USA (Briggs and Mount, 1982; Briggs and Robison, 1984) and rare full-body specimens alongside more common appendages were described from the Chengjiang Biota in China (Chen et al., 1994; Hou et al., 1995).

It is during the last 20 years that new occurrences of Radiodonta started to accumulate at a rapid rate, giving a comprehensive view on the evolution and paleoecology of the group. Key studies by Kühl et al. (2009) and Daley et al. (2009) used a phylogenetic approach to situate radiodonts in the lower stem lineage of Euarthropoda, indicating that their anatomical features provide insight into the acquisition of euarthropod morphological features. The identification of large cephalic carapaces in the Burgess Shale radiodont taxa *Hurdia* (Daley et al., 2009; Daley et al., 2013a) and *Cambroraster* (Moysiuk and Caron, 2019), consisting of a central element and two lateral elements (Figures 6A–E) (Supplementary Table S1A), meant that similar isolated carapaces in numerous Cambrian lagerstätten have found a home within Radiodonta (e.g., Sun et al., 2020a; b; Pates et al., 2021b) New discoveries of frontal appendages and oral cones have shown that these two anatomical features are highly variable in morphology within the clade, giving opportunities for reconstructions of their feeding paleoecology (Daley and Peel, 2010; Daley et al., 2013b; Vinther et al., 2014; Cong et al., 2016; Cong et al., 2017; Cong et al., 2018; Lerosey-Aubril and Pates, 2018; Pates et al., 2018; Guo et al., 2019; Pates and Daley, 2019; Pates et al., 2019; Wu et al., 2021a; Wu et al., 2021b; Wu et al., 2022 and references therein). Whole body specimens of radiodonts remain relatively rare but have been instrumental in describing previously unknown features of their flaps, setal blades and tail fan (Van Roy and Briggs, 2011; Van Roy et al., 2015; Zeng et al., 2022), and internal organs such as the nervous system (Cong et al., 2014; Moysiuk and Caron, 2022) and digestive tract (Daley and Edgecombe, 2014; Vannier et al., 2014). Radiodonts are now know from 34 different *lagerstätten* from the paleocontinents of Gondwana, Laurentia, South China, North China, Baltica, and Avalonia (Figure 7), with their total diversity of species standing at 37 named species and several more taxonomically uncertain specimens (Supplementary Datasheet S1 and Supplementary Table S2). It is the aim of this review article to summarize the current knowledge of the Radiodonta clade, focusing on their diversity, distribution and paleogeography, their paleoecology, and their evolutionary significance for understanding arthropod evolution.

2 Materials and methods

Radiodonta publications have been summarized into a table of occurrences (Supplementary Datasheet S1 and Supplementary Table S2), which was used to examine the diversity and paleogeographic distribution of the clade. Photographs of specimens taken by A. Daley were mainly photographed between 2006 and 2014, and were imaged with a Canon EOS 500D digital SLR camera fitted with an EF-S 60 mm f2.9 Macro Lens. Light was orientated at both low and high angles on the specimens, dry and submerged in water. To enhance contrast of those specimens that were highly reflective, a polarizing filter on the camera lens was oriented perpendicular to another polarizing filter at the light source, following the method of Bengtson (2000). Figures and illustration were made using Photoshop and Illustrator Photoshop CS4 (Adobe Systems Inc.) under a University of Lausanne license. The reconstruction map has been produced by using Gplates_2.0.3 software, using Torsvik and Cocks (2017) package.

A variety of terms (Supplementary Table S1) have been used to describe the structures in the body of Radiodonta (Figure 2). In the

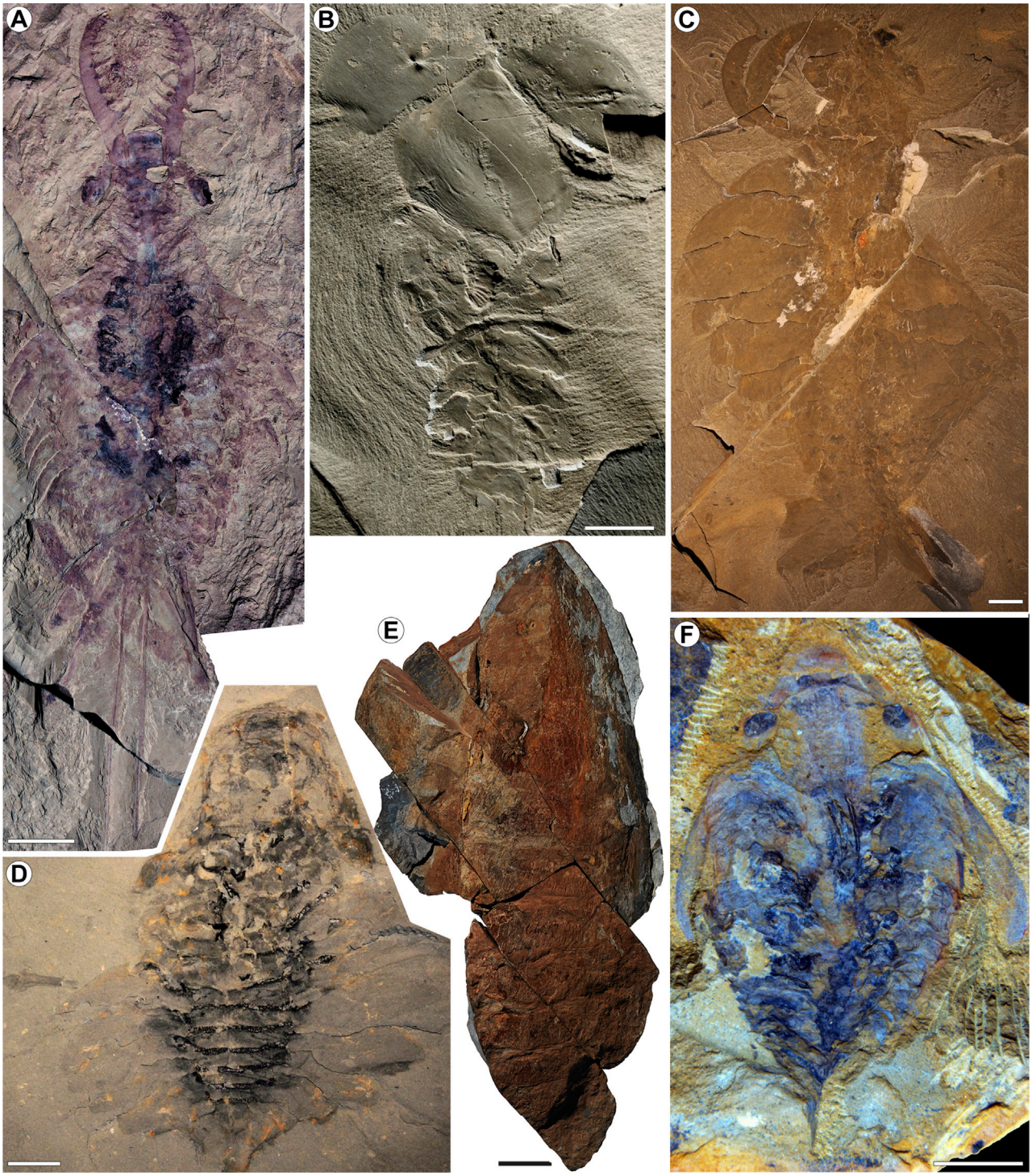

FIGURE 1
Radiodont specimens with whole body preservation. **(A)** *Innovatiocaris maotianshanensis* from the Chengjiang Biota, China, ELRC 20001. Stitched image of part and counterpart. **(B)** *Hurdia triangulata* from the Burgess Shale, Canada, ROM 59252. **(C)** *Anomalocaris canadensis* from the Burgess Shale, Canada, ROM 51214. **(D)** *Peytoia nathorsti* from the Burgess Shale, Canada, USNM 274141. **(E)** *Aegirocassis benmoulai* from the Fezouata Shale, Morocco, YPM 237172. **(F)** *Lyrarapax unguispinus* from the Chengjiang Biota, YKLP 13305. Image credits: **(A–D)** A. Daley, **(E)** P. Van Roy, **(F)** P. Cong. Scale bars are 1 cm in all but **(E)**, where the scale bar is 10 cm.

description below, we follow the terminology of Wu et al. (2022) for the frontal appendages, Liu et al. (2020) for cephalic carapace elements, Daley and Bergström (2012) and Pates et al. (2021a) for the oral cone, Daley and Edgecombe (2014) for structures in the body trunk and the tail fan, and Sheppard et al. (2018) for the vanes in the tail fin.

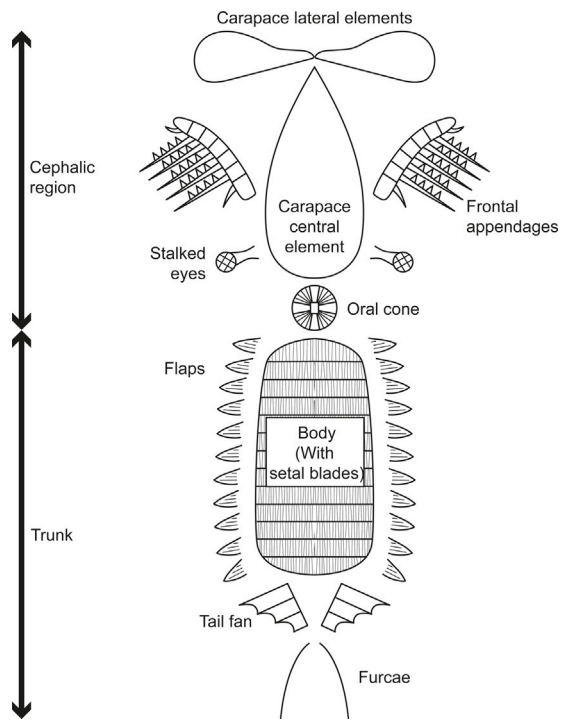

FIGURE 2
Generalized anatomy of radiodonts.

3 Anatomical features and evolutionary significance

Radiodonta has a peculiar morphology within Arthropoda, but shows variabilities within the group that allow many ecological and evolutionary interpretations (Daley and Budd, 2010; Van Roy et al., 2015; Moysiuk and Caron, 2021). A notable feature is their large size range, with total body length varying from 10 mm in the smallest known radiodont *Stanleycaris* from the Burgess Shale (Moysiuk and Caron, 2022), to over 200 cm in length with the giant suspension-feeder *Aegirocassis* from the Fezouata Shale (Van Roy and Briggs, 2011; Van Roy et al., 2015). In this section, we provide an overview of the general morphology of radiodonts, followed by a detailed treatment of the significance of their anatomy for understanding paleoecology and euarthropod evolution.

3.1 General morphology

The order Radiodonta belongs to the class Dinocarida (Collins, 1996), which includes Radiodonta and Opabiniidae, a clade that is not consistently recovered as monophyletic in phylogenetic analyses (Daley et al., 2009; Pates et al., 2022). In general, Radiodonta are bilaterally symmetrical with a non-mineralized cuticle (Collins, 1996; Cong et al., 2016; Liu et al., 2018). The body (Figure 2) is divided in two parts, the anterior cephalic region and the posterior body trunk (Collins, 1996). The unsegmented head has at least one preoral appendage pair and a ventral mouth with radial plates (Collins, 1996). It bears at least one pair of compound eyes, which can be stalked or sessile (Collins, 1996; Paterson et al., 2020; Moysiuk and Caron, 2022). The body trunk is metameric, with laterally-oriented flaps presumably used for swimming and setal blades that are interpreted as the gills (Collins, 1996). The posterior body termination can be tapering to a blunt end, or can have a tail fan consisting of multiple vanes (Collins, 1996).

The preoral frontal appendages (Figures 4, 5) (Collins, 1996; Cong et al., 2016; Liu et al., 2018) consist of podomeres separated by arthrodial membranes, with ventral spine-like structures or blades called endites (Supplementary Table S1B) on at least five of the podomeres (Cong et al., 2016; Liu et al., 2018; Edgecombe, 2020). The appendage is divided into three regions: the proximal podomeres, on which there may be a simple endite (Cong et al., 2016; Lerosey-Aubril and Pates, 2018; Wu et al., 2022); the intermediate podomeres bearing a series of elongated and laminiform endites that can have auxiliary spines lining the anterior and/or posterior margins (Cong et al., 2016; Lerosey-Aubril and Pates, 2018); and the distal podomeres, which can also bear endites that are short and reduced compared to the intermediate ones (Cong et al., 2016; Lerosey-Aubril and Pates, 2018; Wu et al., 2022).

The oral cone (Figure 3) consists of a radial arrangement of plates (Supplementary Table S1C), sometimes bearing spines that face inwards into a central opening (Collins, 1996; Daley and Bergström, 2012). Oral cones often have either three (triradial oral cone, as seen in *Anomalocaris*, Figure 3I) or four (tetraradial, as seen in *Hurdia* and *Peytoia*, Figures 3A–C,E) large plates. The small and large plates can be adorned with scale-like nodes or marginal furrows (Daley and Bergström, 2012; Zeng et al., 2017) in the triradial oral cones, and in some unusual oral cones that show a mix of features of the tetraradial and triradial forms (Figures 4J,K) (Zeng et al., 2018; Sun et al., 2020a). *Hurdia* has inner rows of teeth within the central opening (Daley et al., 2009; Daley et al., 2013a). Some radiodonts do not possess an oral cone, but have gnathobase-like structures (GLSs) and a set of smooth and tuberculate plates not clearly arranged in a radial fashion (Figures 3F–H) (Cong et al., 2017; Cong et al., 2018).

The head of most radiodonts bears a cephalic carapace (Supplementary Table S1A) of variable morphology. These are enlarged in Hurdiidae and Tamisiocaridiidae (Figures 1B,E, 6A–E), which have a symmetrical and often anteriorly tapering central carapace associated with a pair of lateral carapace elements (Daley et al., 2009; Daley et al., 2013a; Zeng et al., 2017; Moysiuk and Caron, 2019). In *Hurdia*, these extend forward from the anterior margin of the head, based on the position of the eyes that have their stalks extruding through ocular notches of the posterior margins of central and lateral elements. The entire carapace complex is nearly as long as the rest of the body but does not cover it completely (Daley et al., 2009; Daley et al., 2013a). The structure of the cephalic carapaces consists of two layers of cuticle (Daley et al., 2013a; Zeng et al., 2017), and often show a reticulate polygonal ornamentation (Van Roy and Briggs, 2011; Daley et al., 2013b). Cephalic carapaces are smaller and more poorly known in Amplectobeluidae and Anomalocarididae, but central and lateral elements have been described in

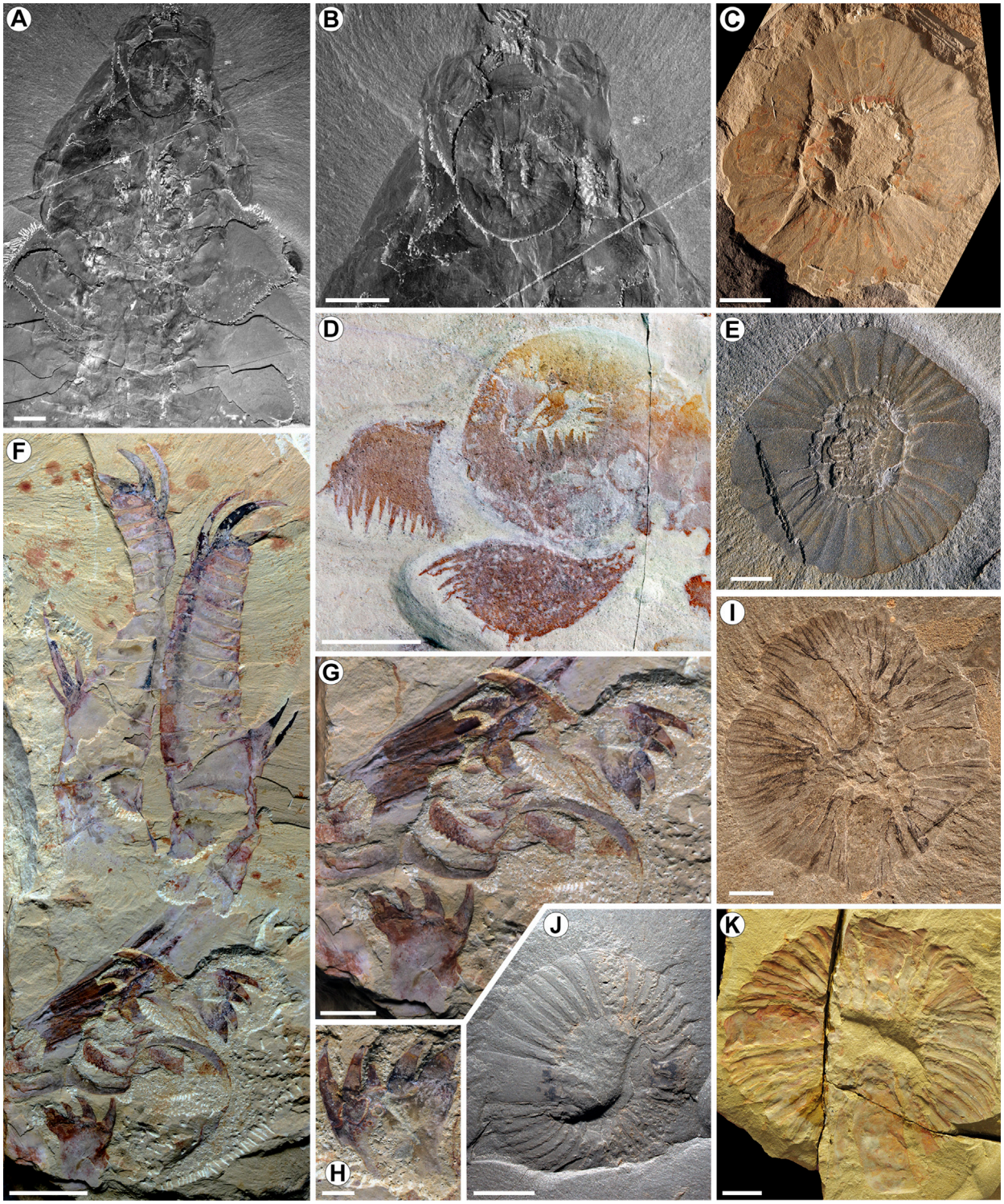

FIGURE 3
Oral structures in Radiodonta. **(A–B)** Oral cone of *Peytoia nathorsti* from the Burgess Shale. USNM 274143. **(A)** Overview showing the position of the oral cone on the ventral anterior surface of the head. **(B)** Closeup on the tetraradial oral cone. **(C)** *Peytoia nathorsti* oral cone in isolation. USNM 193926. **(D)** *Buccaspinea cooperi* oral cone from the Marjum Formation. BPM 1108a. **(E)** *Hurdia* oral cone from the Burgess Shale, showing inner teeth within the central opening. ROM 59260. **(F–H)** *Amplectobelua symbrachiata* from the Chengjiang biota. YKLP 13889. **(F)** Disarticulated assemblage with appendages, GLSs, and smooth and tuberculate plates. **(G)** Closeup on GLSs and smooth and tuberculate plates. **(H)** Closeup of GLS. **(I)** *Anomalocaris canadensis* triradial oral cone from the Burgess Shale. ROM 61679. **(J)** *Cordaticaris striatus* oral cone from the Zhangxia Formation, North China. NIGPAS 173116. **(K)** Unusual oral cone from the Guanshan Biota. NIGPAS 162529. Image credits: **(A,B)** X. Zhang, Smithsonian NMNH, **(C,E,I)** A. Daley, **(D)** S. Pates, **(F–H)** P. Cong, **(J)** F. Xiao, **(K)** H. Zeng. Scale bars are 10 mm in **(A,B,D,F and K)**, 5 mm in **(C,E,G,I and J)**, 1 mm in **(H)**.

Anomalocaris (Daley and Edgecombe, 2014) and *Amplectobelua* (Cong et al., 2017).

The number of segments in the body varies between taxa, ranging from 7 to 15 or more, with each segment bearing setal blades and one or two pairs of flaps (Supplementary Table S1D). Flaps are triangular in outline and may bear transverse lines in the anterior half or across the whole flap (Daley et al., 2013a). Flaps can be large and distinctly tapering posteriorly, as seen in *Anomalocaris canadensis* (Figure 1C) (Whittington and Briggs, 1985; Collins, 1996; Daley and Edgecombe, 2014), or can be reduced and roughly equal in size along the body, as seen in *Hurdia* (Figure 1B; 6A) (Daley et al., 2013a). The body also bears bands of thin, elongated setal blades (Daley et al., 2009; Daley et al., 2013a). These setal blade bands have been interpreted as being dorsal (Whittington and Briggs, 1985; Bergström, 1986; Van Roy et al., 2015), ventral (Moysiuk and Caron, 2019; Moysiuk and Caron, 2022), or extending out onto the flaps (Daley et al., 2009; Daley et al., 2013a). The posterior termination of the body ends bluntly in some taxa (Figure 1D), but in others there is an elaborate tail fan (Figures 1A,C) (Whittington and Briggs, 1985). When present, the tail fan may consist of up to three pairs of vanes (Collins, 1996; Cong et al., 2016; Sheppard et al., 2018).

3.2 Morphological features enabling paleoecological and paleobiological interpretations

3.2.1 Feeding strategy

All radiodonts are interpreted as marine nektonic predators (Bambach et al., 2007; Dunne et al., 2008; Daley and Budd, 2010; Perrier et al., 2015; Guo et al., 2019). Several features allow us to reconstruct this feeding strategy (Daley and Budd, 2010; Van Roy et al., 2015; Guo et al., 2019; Caron and Moysiuk, 2021). The frontal appendages are interpreted as grasping organs that catch the food and bring it to the mouth (Daley and Budd, 2010). They give information about the feeding strategy, much more than the oral cones, which are less abundant and for which the function, use and movement remain enigmatic, other than their suggested ability to create suction to bring food towards the mouth (Daley and Bergström, 2012; Zeng et al., 2018). Other features of radiodont anatomy that suggest predation are their relatively large body size compared to other Cambrian animals, their streamlined body form adapted for agile swimming, their large complex eyes, and their complex digestive system with large gut diverticulae for efficient food processing (Whittington and Briggs, 1985; Collins, 1996; Usami, 2006; Daley and Budd, 2010; Vannier et al., 2014; Lerosey-Aubril and Pates, 2018; Guo et al., 2019; Paterson et al., 2020).

Various quantitative methods have been employed to analyze the paleoecology of Radiodonta, including hydrodynamic calculations (Usami, 2006), 3D modeling of appendages and their movement (De Vivo et al., 2021; Bicknell et al., 2023), finite element analysis (Bicknell et al., 2023), computational fluid dynamics (Bicknell et al., 2023), and geometric morphometrics of cephalic carapaces (Daley et al., 2013a; Caron and Moysiuk, 2021). The morphology of the frontal appendages allows three main predatory groups to be distinguished: raptorial predators, sediment sifters and suspension-feeders (Daley and Budd, 2010; Vinther et al., 2014; Van Roy et al., 2015; Guo et al., 2019).

The raptorial predation mode was used by members of Anomalocarididae and Amplectobeluidae (Daley and Budd, 2010; Daley et al., 2013b). The appendages of *Anomalocaris canadensis* (Figure 4F) are many-segmented and well-articulated with short endites, enabling them to be mobile, flexible and dexterous, and making them efficient for catching macro-scale prey ranging in size from 20 to 50 mm (Daley and Budd, 2010; De Vivo et al., 2021; Bicknell et al., 2023). The pincer-shape appendage of *Amplectobelua* (Figure 4G) had a low degree of flexibility but could still grasp prey of relatively small sizes at around 20 mm (De Vivo et al., 2021). No radiodonts, even these raptorial taxa, had the ability to regularly consume prey with mineralised exoskeletons, as suggested by Nedin (1999), who envisioned *Anomalocaris* could use a flexing motion to consume mineralised trilobites. Computational modelling has shown that such motions are not possible with *Anomalocaris* appendages (De Vivo et al., 2021), nor was their sclerotised cuticle capable of tearing a mineralised exoskeleton (Bicknell et al., 2023). Damages preserved in trilobite and nektaspid exoskeletons (Conway Morris, 1985; Nedin, 1999) and large coprolites found in Cambrian lagerstätten that contain fragments of trilobites (Nedin, 1999; Vannier and Chen, 2005) had previously been attributed to durophagous predation by radiodonts (Nedin, 1999; Klug et al., 2017; Vinn, 2018; Zong, 2021; Zhang et al., 2023). Based on the unsuitability of the frontal appendage (De Vivo et al., 2021; Bicknell et al., 2023) and oral cone (Daley and Bergström, 2012) for durophagy, Anomalocarididae are no longer considered to have been predators of mineralized shelly taxa, and instead these coprolites and damages are attributed to *Redlichia* and other Cambrian trilobites (Daley et al., 2013b) or gnathobase-bearing artiopodan euarthropods (Bicknell et al., 2018; 2022). The Amplectobeluidae taxon *Guanshancaris* has been suggested to have been capable of durophagy, based on its flexible proximal endites and the stout nature of the endites on intermediate podomeres, with suggested prey being trilobites and brachiopods, which show damage to their exoskeleton in specimens found closely associated with *Guanshancaris* (Zhang et al., 2023). Anomalocarididae and most Amplectobeluidae taxa likely consumed soft-bodied and lightly sclerotized prey items (Daley and Bergström, 2012; De Vivo et al., 2021; Bicknell et al., 2023), with *Guanshancaris* potentially being capable of durophagy (Zhang et al., 2023).

The frontal appendages of all Hurdiidae and several Tamisiocarididae are characterised by the presence of elongated, straight, laminiform endites in the intermediate region (Collins, 1996; Daley and Budd, 2010; Lerosey-Aubril and Pates, 2018; Guo et al., 2019; Wu et al., 2022). Radiodonts possessing these appendages are interpreted to be either sediment sifters or filter feeders (Daley and Budd, 2010; Vinther et al., 2014; Van Roy et al., 2015). The main differences between them are related to the shape, position, and distribution of the auxiliary spines (Caron and Moysiuk, 2021). In sediment-sifter radiodonts, such as *Hurdia* and *Peytoia* (Figures 4A–C), the auxiliary spines are thick, relatively widely spaced and short (Caron and Moysiuk, 2021),

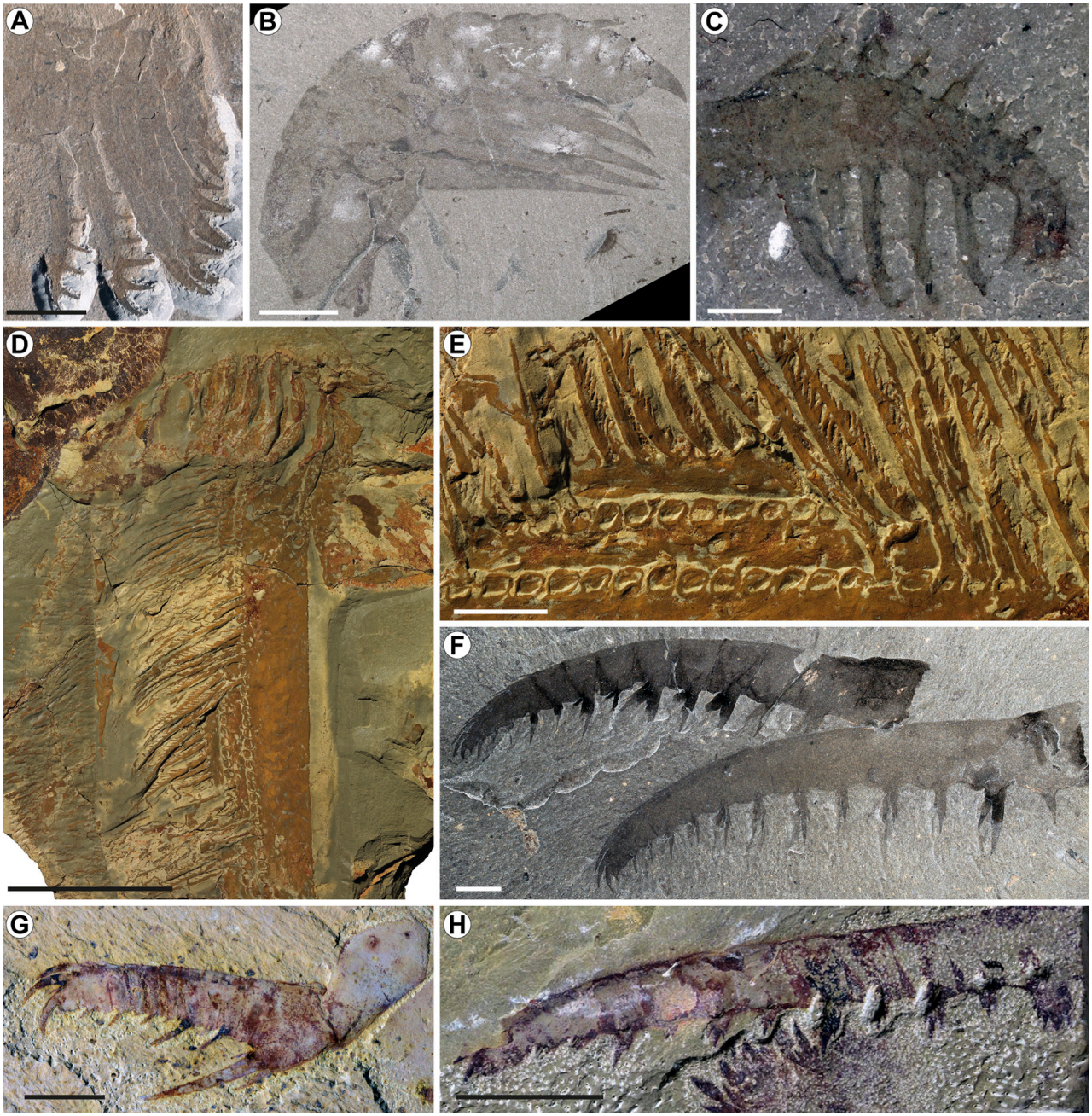

FIGURE 4
Frontal appendages of Hurdiidae, Anomalocarididae and Amplectobeluidae. **(A–E)** Hurdiidae. **(A)** *Hurdia victoria* frontal appendage from the Burgess Shale, Canada. ROM60020. **(B)** *Peytoia nathorsti* from the Burgess Shale, Canada. ROM60036. **(C)** *Stanleycaris hirpex* from the Burgess Shale. ROM 59944, holotype. **(D–E)** *Aegirocassis benmoulai* from the Fezouata Shale, Morocco. YPM 527125, paratype. **(D)** Whole hurdiid appendage. **(E)** Closeup showing setae and sockets. **(F)** Anomalocarididae. *Anomalocaris canadensis* from the Burgess Shale, Canada. ROM 62543. **(G–H)** Amplectobeluidae. **(G)** *Amplectobelua symbrachiata* from the Chengjiang biota, YKLP 13313. **(H)** *Ramskoeldia platyacantha* from the Chengjiang Biota, YKLP 13325, holotype. Image credits: **(A–F)** A. Daley. **(G–H)** P. Cong. Scale bars are 10 cm in **(D)**, 50 mm in **(E,G and H)**, 10 mm in **(B,C and F)**, 5 mm in **(A)**.

lending a robustness useful when sieving sediment (Caron and Moysiuk, 2021). These appendages are less dexterous than the raptorial predator appendages, and might have been used with both appendages in concert to surround and capture prey (De Vivo et al., 2021). The presence of medial spines (referred to as gnathites) in *Peytoia* (Daley et al., 2013a) and *Stanleycaris* (Moysiuk and Caron, 2021) could have aided in holding, stabbing and tearing soft-bodied prey items, with a suggestion that durophagy on mineralized shelly prey might have been possible for *Peytoia* (Moysiuk and Caron, 2021).

Sediment sifters are further divided in two categories (Caron and Moysiuk, 2021). Macrophagous sediment sifters such as *Hurdia* and *Peytoia* are adapted for large prey items (60–100 mm and 20–40 mm respectively; see De Vivo et al., 2021), while the microphagous ones,

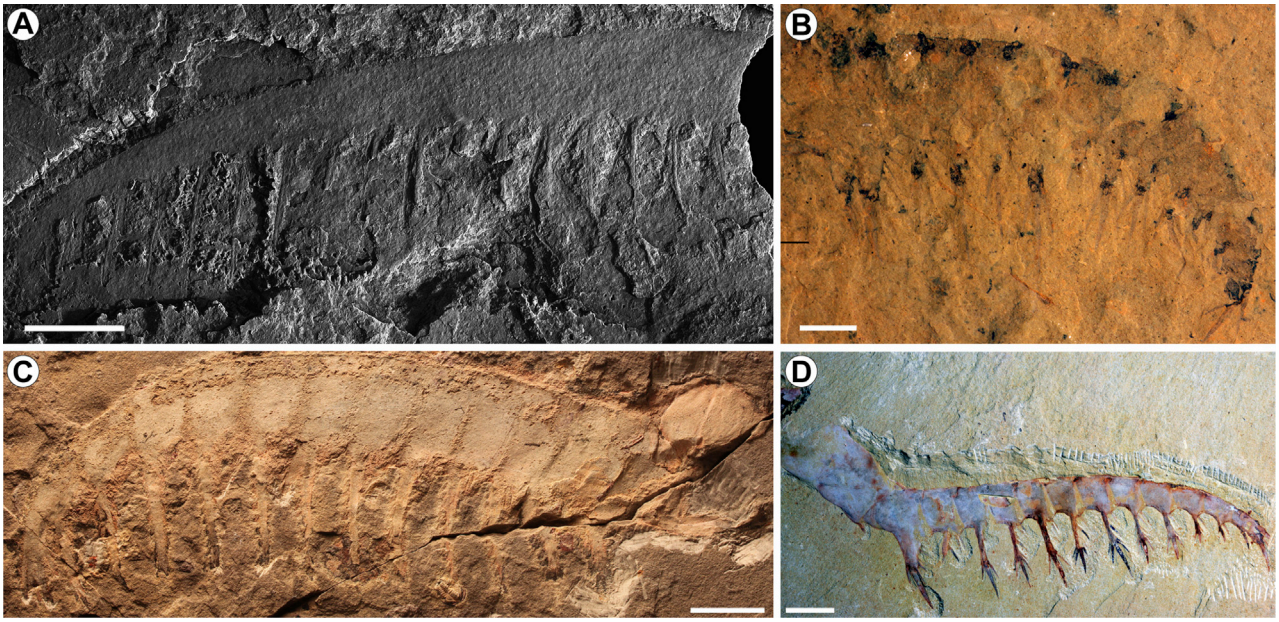

FIGURE 5
Frontal appendages of Tamisiocarididae. **(A)** *Tamisiocaris borealis* from the Sirius Passet, Greenland. MGUH 29154, holotype. **(B)** *Houcaris magnabasis* from the Comet Shale Member of the Pioche Formation, Nevada, USA. KUMIP 293584, holotype. **(C)** "*Anomalocaris*" *briggsi* from the Emu Bay Shale, Australia. SAM P40180, holotype. **(D)** *Houcaris saron* from the Chengajiang Biota, China. YKLP 13459. Image credits: **(A)** J. Peel. **(B)** S. Pates. **(C)** A. Daley. **(D)** P. Cong and S. Pates. Scale bars are all 10 mm.

including *Cordaticaris*, *Titanokorys*, and questionably *Cambroraster* are adapted for smaller prey items (Caron and Moysiuk, 2021; De Vivo et al., 2021). The difference between them is based on the interspace and the number of the robust auxiliary spines, with microphagous sediment-sifters having less interspace and a larger number of auxiliary spines than macrophagous sediment-sifters (Caron and Moysiuk, 2021). According to De Vivo et al. (2021), the appendage of *Cambroraster* could be more suitable for the suspension-feeding strategy.

Suspension-feeders differ from microphagous sediment-sifters by the strongly specialized auxiliary spines, or setae, that are much longer than the height of endite to which they attach (Vinther et al., 2014; Van Roy et al., 2015). The setae are often numerous and densely-packed, and the interspace, called mesh size, is small, such that they effectively create a net to catch plankton (Vinther et al., 2014; Van Roy et al., 2015). Suspension feeding taxa include *Aegirocassis* (Figures 4D,E) and *Tamisiocaris* (Figure 5A), and questionably "*Anomalocaris*" *briggsi* (Figure 5C), *Pahvantia* and *Cambroraster* (Vinther et al., 2014; Van Roy et al., 2015; Lerosey-Aubril and Pates, 2018; Paterson et al., 2020; Caron and Moysiuk, 2021; De Vivo et al., 2021). In *Aegirocassis*, another order of spinosity is observed in the form of spinules that attach to the setae (Figures 4D,E) (Van Roy et al., 2015).

Oral cones or other comparative structures (e.g., gnathobase-like structures, GLSs) have a lower preservation potential than frontal appendages, and are found infrequently in the fossil record (Daley and Bergström, 2012; Zeng et al., 2018). Only 13 taxa (*Amplectobelua*, *Anomalocaris*, *Buccaspinea*, *Cambroraster*, *Cordaticaris*, *Hurdia*, *Innovatiocaris*, *Lyrarapax*, *Peytoia*, *Ramskoeldia*, *Stanleycaris*, *Titanokorys*, maybe *Guanshancaris kunmingensis*) have their oral cones described so far, and it is not possible to link specific characters with any particular feeding strategy (Collins, 1996; Daley and Bergström, 2012; Daley et al., 2013a; Paterson et al., 2016; Cong et al., 2017; Cong et al., 2018; Liu et al., 2018; Zeng et al., 2018; Moysiuk and Caron, 2019; Sun et al., 2020a; Caron and Moysiuk, 2021; Moysiuk and Caron, 2021; Zeng et al., 2022). Oral cones share the same main characteristic of slightly overlapping plates surrounding a central opening, with variations in organization that change the symmetry of the oral cone. The combinations of features are so unique for each described oral cone morphology that identifying the ecological function to determine a feeding strategy remains impossible. However, the *Anomalocaris* oral cone has been interpreted to employ a suction mechanism and not a crushing one (Daley and Bergström, 2012; Zeng et al., 2018).

The cephalic carapaces may also play a role in the feeding ecology of various radiodont taxa, most notable in the Hurdiidae where carapaces are enlarged and complex (Figure 6A). Sediment sifters may have used their protruding cephalic carapaces to disturb the sediment that is then sifted by the frontal appendages, and/or to help trap prey and funnel it towards the mouth (Daley et al., 2009; Daley et al., 2013a; Moysiuk and Caron, 2019). Liu et al. (2020) compared the large cephalic carapace of *Cambroraster* to that of horseshoe crabs and trilobites that feed on infaunal organisms, with the cephalic carapace providing a protective dome for movement of the appendages to search for prey in the sediment. This suggests a eudemersal mode of life for *Cambroraster* and perhaps all hurdiids (Liu et al., 2020), and radiodonts in general have

been considered to be eudemersal in large-scale analyses of the evolution of the nekton (Klug et al., 2010; Whalen and Briggs, 2018). The smaller cephalic carapaces of Amplectobeluidae and Anomalocarididae likely served a protective function, rather than being implemented in feeding (Daley and Edgecombe, 2014; Cong et al., 2016; Cong et al., 2017; Cong et al., 2018). Using a phylomorphospace approach, Caron and Moysiuk (2021) show that there are no statistically significant correlations between cephalic carapace element shape and feeding strategy when comparing microphagous and macrophagous sediment sifters, and suspension feeders (Caron and Moysiuk, 2021). However, their analyses did reveal that microphagous sediment-sifters have on average a larger body size than any other group of radiodonts (Caron and Moysiuk, 2021). An extreme example is the giant microphagous suspension feeder *Aegirocassis*, which is one example of the repeated evolution of gigantism in microphagous animals seen also in whales, fish, sharks and rays (Friedman et al., 2010; Marx and Uhen, 2010; Van Roy et al., 2015; Pimiento et al., 2019; Mironenko, 2020).

3.2.2 Swimming

All radiodonts were nektonic active swimmers (Usami, 2006; Daley et al., 2013a; Van Roy et al., 2015; Sheppard et al., 2018; Zeng et al., 2022). Propulsion was provided by movement of the flaps (Usami, 2006; Daley et al., 2013a; Van Roy et al., 2015), likely in a single synchronized wave, comparable to the swimming behavior of living manta rays (Usami, 2006). *Anomalocaris* (Figure 1C) is interpreted to have been an agile swimmer, well adapted for hunting, based on the width of the flaps and the hydrodynamic shape of the body overall (Usami, 2006; Daley et al., 2013a). In contrast, *Hurdia* (Figures 1B, 6A) had reduced flaps and a more convex rounded body, making it less well adapted for agile swimming in the water column, instead suggesting it was nektobenthic (Daley et al., 2013a). *Cambroraster* also has reduced flaps and a similar body shape to *Hurdia* (Moysiuk and Caron, 2019), and based on the shape of its cephalic carapace, Liu et al. (2020) suggested it had a eudemersal ecology. The 2 m-long hurdiid *Aegirocassis* (Figure 1E) is peculiar because it has two pairs of relatively small flaps, the ventral and dorsal flaps (Van Roy et al., 2015). It is considered an agile swimmer, however, and only the ventral pairs of flaps were used for swimming propulsion, while the dorsal flaps played a role in stabilization and steering (Van Roy et al., 2015). This configuration is best adapted to maintaining a steady speed over long distances or time, matching its interpreted feeding ecology as a suspension feeder (Van Roy et al., 2015).

The tail fan present in some radiodonts such as *Anomalocaris* and *Innovatiocaris* (Figures 1A,C) may also have been used during swimming (Usami, 2006; Sheppard et al., 2018; Zeng et al., 2022). According to Sheppard et al. (2018), the tail fan could generate forces for various swimming maneuvers, such as changing direction, but was not used for propulsion (Sheppard et al., 2018). A unique feature of the tail in *Innovatiocaris* is the presence of a pair of elongated, thin furcae, which have a currently unknown function (Chen et al., 1994; Zeng et al., 2022).

3.2.3 Respiration

In radiodonts, the respiratory exchange between the environment and the animal has been linked to the setal blades (Whittington and Briggs, 1985; Daley et al., 2013a; Daley and Edgecombe, 2014; Van Roy et al., 2015). Their structure as a multitude of thin, flexible structures covering a large part of the body trunk seems to be well adapted for increasing surface area. They were used in ion and oxygen exchange, and the presence of lamellae on the two sides of each setal blade in *Aegirocassis* reinforced this interpretation because it would give even more surface area for exchange (Van Roy et al., 2015). The lamellae could also serve to help lock adjacent setal blades together and make the band of setal blades a cohesive unit (Van Roy et al., 2015), helping to explain their consistent preservation as complete blocks of setal blades (Daley et al., 2009; Daley et al., 2013a; Daley et al., 2013b). Their exact orientation and relation with the flaps remain debated, with some specimens seeming to have them located dorsally (*Peytoia*, and *Aegirocassis* for example; Figures 1D,E) (Van Roy et al., 2015), while in other taxa they were interpreted as being more closely associated with the flaps (*Hurdia*; Figures 1B, 6A) (Daley et al., 2009; Daley et al., 2013a). In *Cambroraster* and *Stanleycaris* (Figure 4C) they are suggested to be ventral (Moysiuk and Caron, 2019; Moysiuk and Caron, 2022). More information is needed to clarify the exact location, attachment, and arrangements of setal blades within radiodonts.

3.2.4 Moulting and development

Ecdysozoa and especially arthropods, with their biomineralized exoskeleton, produce moults as they grow (Daley and Drage, 2016; Drage and Daley, 2016; Drage, 2019; Drage et al., 2019; Drage, 2022). The process of moulting, also called ecdysis, is crucial for the ontogenetic development of individuals and is also used for repair and regeneration after injuries, even if the process of moulting leaves the animal temporarily immobile and vulnerable in the absence of the protective hardened or sclerotised exoskeleton (Daley and Drage, 2016; Drage, 2019; Drage, 2022). Arthropod moulting has been well studied in the fossil record (Daley and Drage, 2016), especially in trilobites (Drage et al., 2018a; Drage et al., 2018b).

Belonging to Arthropoda and more generally to Ecdysozoa, radiodonts should moult their external cuticle as they grow (Daley et al., 2013a), but few targeted studies on moulting and ontogenetic development within radiodonts have been possible (Liu et al., 2018). Nonetheless, disarticulated assemblages do provide some information possibly linked to moulting. *Hurdia* disarticulated assemblages are found repeatedly in the same relative orientation, which is thought to be linked to moulting behavior (Daley et al., 2013a). *Anomalocaris canadensis* displays two different preservational modes of the body trunk, either as cuticle with the wide swim flaps, or as a series of closely arranged bands of setal blades, which are rarely found together in the same specimen (Daley and Edgecombe, 2014). It was suggested that these two modes result from disarticulation of the body from the ventral flaps, perhaps owing to moulting, or for a taphonomic reason such as differential decay rates (Daley and Edgecombe, 2014).

In the Fezouata Shale, high concentrations of *Aegirocassis* remains have been found together (Van Roy et al., 2015), suggesting that *Aegirocassis* was living in groups and moulting close to the seafloor. This could be compared to interpretations of

mass moulting behavior seen in other fossil arthropods, such as eurypterids (Braddy, 2001; Vrazo and Braddy, 2011) and trilobites (Daley and Drage, 2016). Notably, mass moulting has already been described in the Fezouata Shale for the trilobite *Symphysurus ebbestadi* (Drage et al., 2019).

There has been no indication in the anatomy of specimens about the process of moulting in radiodonts. The location of the ecdysial suture and the timing of moulting remain unknown. The description of a juvenile *Lyrarapax* specimen from the Chengjiang Biota showed that it possessed an oral cone (Liu et al., 2018), while the adult specimens do not show evidence of having any circumoral plates (Cong et al., 2014; Cong et al., 2016). This either indicates that the lack of an oral cone in adults is a taphonomic effect, as suggested by Liu et al. (2018), or it could indicate that anatomy of radiodonts can change during growth, suggesting the possibility of indirect development in this group. However, broadly speaking, the major morphology seems to be similar between specimens of different sizes for radiodonts known from large numbers of specimens (Daley et al., 2013a; Moysiuk and Caron, 2019).

3.2.5 Colonized radiodonts

In early Paleozoic communities, arthropods were some of the biggest animals of their communities (Edgecombe, 2020), and this is particularly true for Radiodonta, especially *Anomalocaris* and the giant *Aegirocassis* (Daley and Budd, 2010; Van Roy and Briggs, 2011; Van Roy et al., 2015; Lerosey-Aubril and Pates, 2018; Caron and Moysiuk, 2021). These large carcasses, and particularly the cephalic carapaces of hurdiid radiodonts, show evidence of having been colonized by other organisms for different types of symbiosis or after death of the animal (Mángano, 2011; Mángano et al., 2012; Mángano et al., 2019). In radiodonts, Daley et al. (2013a) reports traces in different carapace elements of *Hurdia*, comparable to traces found in other non-radiodont Cambrian arthropod carapaces including *Tuzoia* from the Burgess Shale and a *Tegopelte*-like arthropod from the Sirius Passet (Mángano, 2011; Mángano et al., 2012; Mángano et al., 2019). The cephalic carapaces of the giant *Aegirocassis* show evidence of attached brachiopod epibionts (Saleh et al., 2022b), as do *Ampyx* and other large trilobites from the same locality (Vidal, 1998). The remains of *Aegirocassis* have been illustrated (drawing by Madmeg, figure 8 in Lefebvre et al., 2016) as a possible habitat for a complete ecosystem, comparable to the ichthyosaur carcass-falls documented in the Toarcian (Posidonia Shale) or with whale-falls today (Dick, 2015; Smith et al., 2015).

3.3 Key insights into euarthropod evolution from Radiodonta

Most phylogenetic analyses situate Radiodonta as a clade in the lower stem lineage to Euarthropoda (Figure 8), as discussed in section 5 below. Radiodont anatomy has therefore been used to help understand arthropod evolution, with the clade showing several first appearances of modern arthropod features and characteristics (Edgecombe, 2020).

3.3.1 Biramous limb evolution

A key feature of euarthropods is that their post-antennal limbs were biramous, referring to a limb that consists of an inner walking branch (endopod) and an outer filamentous branch (exopod), attached via a limb base or protopod (Boxshall, 2013). The morphology of the radiodont body trunk, with its lack of walking limbs and the presence of setal blades and associated flaps, has been interpreted as an early stage in the evolution of the euarthropod biramous limb, because the setal blades of taxa such as *Hurdia* and *Aegirocassis* bear a remarkable similarity to the respiratory branch, or exite, of trilobite biramous limbs (Daley et al., 2009). Sitting just below Radiodonta in the euarthropod stem lineage, the gilled lobopodians *Kerygmachela* and *Pambdelurion* from Sirius Passet possess both lobopodous walking limbs and flaps (Budd, 1998a; Budd, 1998b). In Radiodonta, key insight came from the discovery of *Aegirocassis* from the Fezouata Biota, which has two pairs of flaps per body segment (Van Roy et al., 2015). The more dorsal pair of flaps is homologous to the flaps seen in gilled lobopodians, and its close association with setal blades indicates that these two structures together are homologous to the exopod branch of the Cambrian biramous limb (Van Roy et al., 2015). The ventral pair of flaps is homologous to the walking limbs of gilled lobopodians and the endopod of the Cambrian biramous limb (Van Roy et al., 2015). The modification from walking limb to flap morphology presumably represents a morphological adaptation to a swimming mode of life within Radiodonta as a whole. Other taxa such as *Peytoia* and *Hurdia* show possible evidence of having two pairs of flaps, although this is not universally the case and some radiodonts, such as *Anomalocaris*, may have lost the dorsal pair of flaps and have only setal blades remaining (Van Roy et al., 2015). The evolutionary transition proceeds further up in the euarthropod stem lineage, with the fusion of these two structures into a biramous limb, as seen in the non-radiodont arthropod *Erratus sperare* from the Chengjiang biota of China (Fu et al., 2022), which possesses lateral radiodont-like flaps and closely associated ventral subconical endopods. This is an intermediate stage between the two pairs of flaps seen in radiodonts, with a flap and endopod in *Erratus*, before we see exopod and endopod in the Cambrian biramous limb in rest of the upper stem lineage to Euarthropoda.

3.3.2 Eyes and vision in radiodonts

The word "eye" refers to organs that have photoreceptors that transform light into a signal that passes through a series of neurons to give visual characteristics of the environment to the taxon (Strausfeld et al., 2016). Within arthropods, eyes have various morphologies today, and the fossil record provides key information for understanding their evolution (Strausfeld et al., 2016). In radiodonts, eyes are prominent in several species, for example, in *Anomalocaris*, *Hurdia* (Figures 6A,B), *Innovatiocaris*, *Lyrarapax* and *Peytoia* (Whittington and Briggs, 1985; Collins, 1996; Daley et al., 2009; Paterson et al., 2011; Cong et al., 2014; Daley and Edgecombe, 2014; Strausfeld et al., 2016; Paterson et al., 2020; Zeng et al., 2022). Most radiodonts possess stalked compound eyes that are relatively large and mobile, protruding from the dorsolateral side of the head (Paterson et al., 2011; Strausfeld et al., 2016). In *Anomalocaris* from the Emu Bay Shale (Figures 6F–H), the eyes found measure 2–3 cm and are composed of a multitude of hexagonally shaped lenses, with at least 16,000 lenses on the

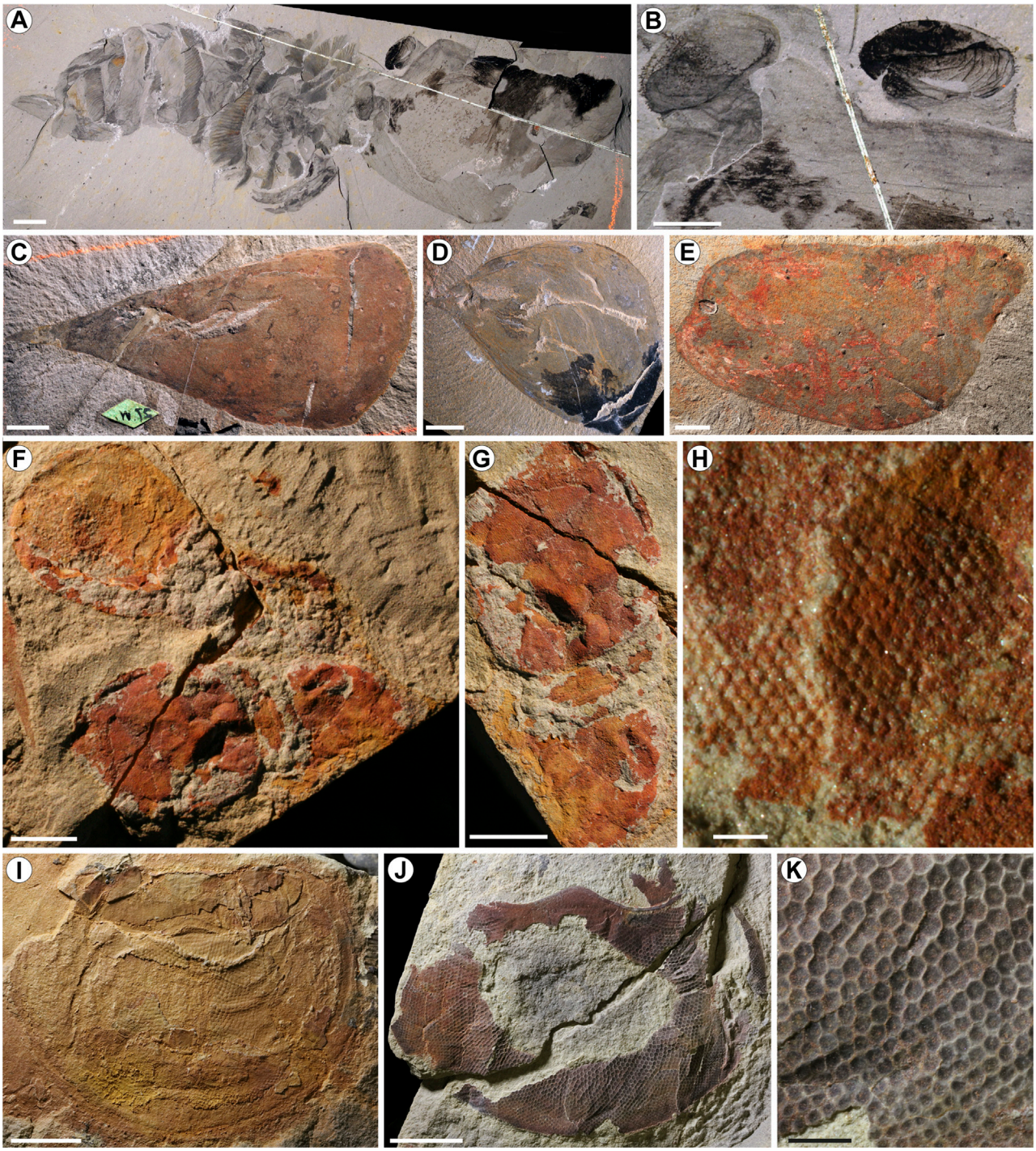

FIGURE 6
Radiodont cephalic structures with importance for understanding the evolution of Euarthropoda. **(A–B)** *Hurdia victoria* from the Burgess Shale, showing the enlarged cephalic carapace with the eyes on stalks protruding from the ocular notches of the central and lateral carapace elements. USNM 274159. **(A)** Whole specimen in lateral view. **(B)** Closeup on the eyes and their relation to the cephalic carapace. **(C)** Central cephalic carapace element of *Hurdia victoria* from the Burgess Shale. USNM 57718, holotype. **(D)** Central cephalic carapace element of *Hurdia triangulata* from the Burgess Shale. USNM 57721, holotype. **(E)** Lateral cephalic carapace element of *Hurdia* from the Burgess Shale. USNM 274159, previous holotype of *Proboscicaris* (now synonymised with *Hurdia*). **(F–H)** Compound stalked eye of *Anomalocaris* aff. *canadensis* from the Emu Bay Shale, Australia. SAM P45920. **(F)** View showing both eyes. **(G)** Closeup on the lower of the two eyes. **(H)** Closeup showing the ommatidia. **(I–K)** Sessile acute zone-type eye of "*Anomalocaris*" *briggsi* from the Emu Bay Shale, Australia. **(I)** SAM P48377. **(J)** Eye of P54853. **(K)** Closeup of the ommatidia in P54853. Image credits: **(A–E)** A. Daley. **(F–K)** J. Paterson. Scale bars are 10 mm in **(A and C–E)**, 5 mm in **(B,F,G,I and J)**, 1 mm in **(K)** and 0.3 mm in **(H)**.

retina surface that is 21.8 cm long and 12.2 cm wide (Paterson et al., 2011; Strausfeld et al., 2016). Such compound eyes have modern analogues with mantis shrimp, dragonflies and rotter flies (Strausfeld et al., 2016). Its large visual surface and stalked morphology make *Anomalocaris*'s eyes larger than the eyes of any living arthropod, and only a few eurypterids and thylacocephalans have larger eyes in the fossil record (Strausfeld et al., 2016; Paterson et al., 2020). The eyes of *Lyrarapax unguispinus* have also been suggested to have an ommatidia morphology, which means that the retina units are arranged in long columns (Cong et al., 2014; Strausfeld et al., 2016). According to Paterson et al. (2011) and Strausfeld et al. (2016), radiodonts have the oldest known compound eye in the fossil record. This eye morphology is particularly well suited for an active predatory lifestyle (Paterson et al., 2020). In contrast to most radiodonts, "*Anomalocaris*" *briggsi* from the Emu Bay Shale has sessile compound eyes that are not on stalks (Figures 6I–K), as revealed by the study of the acute-zone of the specimens (Paterson et al., 2020). Previously, the radiodont eye morphology was said to have been the ancestral eye pattern for the phylum (symplesiomorphic character), which some of the previously cited living predators still display today (Strausfeld et al., 2016; Paterson et al., 2020). This sessile morphology, which would be suitable to a filter-feeding lifestyle, could be an apomorphy in radiodonts, (Paterson et al., 2020).

A new hypothesis emerged in the radiodont body plan with the discovery that a median structure in the head of *Stanleycaris* from the Burgess Shale may represent a third eye (Moysiuk and Caron, 2022). *Stanleycaris* is described as possessing the typical pair of radiodont stalked eyes, and a sessile median eye situated in a head lobe (Moysiuk and Caron, 2022). Similar structures in other radiodonts, such as in *Peytoia* and *Lyrarapax*, were suggested to also represent third eyes (Moysiuk and Caron, 2022). Restudy of purported median structures in these and other radiodont taxa is required to confirm the presence of a third eye across Radiodonta. A median eye is already known in Opabinidae, a closely related clade of stem lineage euarthropods, which possess five stalked eyes (Whittington, 1975; Moysiuk and Caron, 2022; Pates et al., 2022). It is also known from *Kylinxia* from the Chengjiang biota, so having it in other Cambrian taxa could show a continuity in median eye evolution (Zeng et al., 2020; Moysiuk and Caron, 2022).

3.3.3 Architecture of the euarthropod head

The cephalic architecture of radiodonts have provided information relevant to discussions of the crown group euarthropod head (Ortega-Hernández, 2015; Zeng et al., 2018; Budd, 2021). Debate exists about the exact nature of ventral plates in the head of modern euarthropods, mostly centered around the labrum and hypostome, and the identification of homologous structures in Cambrian fossil arthropods, and the broader implications for understanding the structure and evolution of the nervous system within the phylum (as discussed below).

In Radiodonta, much of the focus has been on the cephalic carapaces, the most prominent of which are the enlarged central and lateral elements of hurdiids (Daley et al., 2009; Daley et al., 2013a; Moysiuk and Caron, 2019; Budd, 2021). Central cephalic elements have also been identified in *Amplectobelua symbrachiata* (Cong et al., 2017), *L. unguispinus*, *Lyrarapax trilobus* (Cong et al., 2014; Liu et al., 2018), *Innovatiocaris maotianshanensis* (Zeng et al., 2022) and *Anomalocaris canadensis* (Daley and Edgecombe, 2014), and lateral elements are known for at least *A. symbrachiata* and *L. unguispinus* (Cong et al., 2017; Liu et al., 2018). The structures described as eyes in certain disarticulated specimens of *Anomalocaris canadensis* (Daley and Edgecombe, 2014) were alternatively interpreted as lateral carapace elements by Moysiuk and Caron (2019).

Debates about the cephalic carapaces in Radiodonta center around whether they are dorsal or ventral in position, which changes their interpretation and suggested homologies with plates seen in the heads of upper stem lineage and crown group euarthropods. For example, the rounded central cephalic structure in *Anomalocaris canadensis* (Figure 1C) was interpreted as dorsal by Daley and Edgecombe (2014), and a carapace of similar size, shape and position observed in *I. maotianshanensis* (Figure 1A) from the Chengjiang Biota (Chen et al., 1994; Wu et al., 2021a; Zeng et al., 2022) is also suggested to be dorsal. However, Budd (2021) suggested that these rounded central carapaces are actually ventral, and further suggested the presence of a ventral sclerite in *Peytoia* (Figure 1D) (Whittington and Briggs, 1985; Collins, 1996), although confirmation awaits a complete redescription of this taxon. Budd (2021) also reinterpreted the structures originally described as lateral carapace elements in *Amplectobelua* (Cong et al., 2017) as ventral structures, and suggested that all these supposedly ventral structures could be considered as homologous to the hypostome of euarthropods. Other interpretations suggest the carapaces of the radiodont head could be homologous to the anterior sclerite seen in upper stem lineage euarthropods as a distinct segment closely associated with the eyes (Ortega-Hernández, 2015; Aria et al., 2020), based on comparisons to the presence of a structure in the anterior region of *Lyrarapax* (Figure 1F) (Liu et al., 2018) and linked to arguments about the organisation of the nervous system of radiodonts (Ortega-Hernández, 2015), however little confirmed evidence for this exists in the fossils (Budd, 2021).

Determining the dorsal or ventral aspect of radiodont cephalic carapaces is plagued by difficulties associated with the flattened nature of these fossils. The break between part and counterpart can pass unevenly through the different body layers, making it difficult to determine the relative positions of structures in the body, further compounded by variable compaction rates and differential decay that may have played a role in disarticulation of the body elements (see discussion in Budd and Daley, 2011). That being said, on balance there seems to be more evidence suggesting that the central carapace elements of radiodonts are dorsal in nature, and that lateral cephalic carapace elements were widespread within the clade. Their exact homologies to sclerites and structures in the euarthropod head remain an open question in the field.

3.3.4 Internal anatomy

Although full body specimens are relatively rare, these have provided a wealth of information about the internal organ organization within radiodonts. Organs are found in the main core of the body, which is round to cylindrical, segmented, and bearing the flaps on the lateral or ventral surface (Figure 2). Internal organs for which there is information include the digestive system, nervous system, and musculature.

3.3.4.1 Digestive system

Anomalocaris canadensis preserves the most complete known digestive system within Radiodonta, and along with partial information from numerous taxa, allows for a general description of the alimentary tract. The radiodont digestive system consists of a simple and straight tube that passes from the oral cone in the head to the anus, which is situated on the most posterior segments of the body, with anteroposterior differentiation into foregut, midgut and hindgut regions (Daley and Edgecombe, 2014). The midgut is typically associated with a series of up to six paired glands or diverticula, which show microstructures and preservation typical of the midgut glands seen in other Cambrian arthropods such as *Leanchoilia*, trilobites, and other taxa in the upper stem lineage of Euarthropoda, as well as the lobopodians and gilled lobopodians lower down in the stem lineage (Vannier et al., 2014).

In *Anomalocaris canadensis* from the Burgess Shale, the foregut and hindgut are relatively wider than the midgut, and both are segmented, with a maximum of six segments in the foregut and four in the hindgut (Daley and Edgecombe, 2014). In contrast, the midgut is thinner than the foregut and hindgut, and is a simple unsegmented tube with a series of paired midgut diverticula located on either side of it. As is typical for Burgess Shale-type preservation (Butterfield, 2002), midgut glands can be variably preserved as round, flat, featureless structures, or higher relief irregular structures preserved in a dark black material, sometimes bearing extremely fine laminations (Daley and Edgecombe, 2014). In the Emu Bay Shale, midgut glands are high relief spherical structures flanking the gut (Daley et al., 2013b). A maximum of six pairs of midgut glands can be identified in the most complete *Anomalocaris canadensis* Burgess Shale specimen (Daley and Edgecombe, 2014).

Other taxa belonging to Amplectobeluidae and Anomalocarididae show similar features for the digestive system. In the Chengjiang Biota taxon *L. trilobus*, segmentation can be seen in the foregut and the midgut is flanked by six pairs of small round glands preserved as darker material (Cong et al., 2016; Liu et al., 2018). However *Amplectobelua* and *Innovatiocaris* from the same locality have undifferentiated simple guts with no associated diverticula (Chen et al., 1994; Zeng et al., 2022). Longitudinal wrinkles and weak segmentation may be visible in the gut of *Innovatiocaris* (Zeng et al., 2022), and the authors suggest that the lack of midguts in this juvenile specimen (Figure 1A) is likely a taphonomic artifact, as compared to the similar situation in the gilled lobopodian *Pambdelurion whittingtoni* (Young and Vinther, 2017), where smaller specimens do not preserve gut diverticula.

Within hurdiids, *Stanleycaris hirpex* (Moysiuk and Caron, 2022) preserves a gut differentiated into a simple foregut and hindgut, and a midgut preserving a series of swellings and constrictions, with some of the swellings bearing parallel laminations that resemble the texture of midgut glands in other Cambrian euarthropods such as *Leanchoilia* (Butterfield, 2002; Moysiuk and Caron, 2022). We note that the specimens figured in Moysiuk and Caron (2022) appear to have paired elongated oval structures arranged in a V-shape preserved as slightly darker or reflective material, potentially representing midgut glands that are closely packed next to the gut (figures 1A, 1D, 1F, 3A, 5L and 5O in Moysiuk and Caron, 2022). Other hurdiid digestive systems include a single partial body specimen of the radiodont *Peytoia* from the Marjum Formation of Utah, USA (Briggs and Robison, 1984; Pates et al., 2018) that preserves a thin, simple unsegmented gut passing along the entire length of the body. A partial fragment of the anteriormost foregut may be preserved in the hurdiid *Cambroraster* from the Burgess Shale (Moysiuk and Caron, 2019), which shows a short tube of soft tissue extending from the oral cone and bearing five rows of small denticles, suggesting that at least some radiodonts had an anterior foregut potentially bearing a circlet of teeth, which has been compared to the minute pharyngeal spinules found in other ecdysozoans (Elzinga, 1998; Smith and Caron, 2015; Moysiuk and Caron, 2019).

Although variably affected by taphonomic processes, there is nothing to discount that the general anatomy of the radiodont digestive system had a stable and consistent anatomy within the clade. When tracked through the euarthropod stem lineage (Figure 8A), the presence of complex gut diverticula flanking the digestive tract evolved first with the larger and more complex lobopodians, such as *Megadictyon* and *Jianshanopodia*, and is then seen in the gilled lobopodians *Kerygmachela* and *Pambdelurion*, the enigmatic *Opabinia*, the radiodont clade, and various Deuteropoda taxa including *Isoxys*, *Leanchoilia*, *Sidneyia*, *Naraoia* and the trilobites (see Vannier et al., 2014). Digestive glands have been described as a major innovation in arthropod evolution because they allow for more efficient absorption of nutrients by increasing the epithelial surface area, allowing the animals to digest larger and more complex food items and facilitating macrophagy. The presence of a complex gut with digestive glands in Radiodonta provides another morphological line of evidence supporting that these large stem lineage arthropods were predators, but unfortunately there has never been a radiodont specimen published that preserves the contents of the guts. We lack direct evidence of their prey items, and must infer this from their frontal appendage anatomy (see Section 3.2.1).

3.3.4.2 Nervous system

Structures interpreted as the nervous system have been described in two radiodonts, and alongside paleoneuroanatomy from other stem lineage euarthropods, these provide conflicting evidence into the nature and evolution of the arthropod head. A contentious debate surrounds whether radiodont frontal appendages are innervated by the protocerebrum, making them homologous to the paired antenniform frontal appendages of living onychophorans and to the euarthropod labrum, or deutocerebral, making them homologous to the antennae, chelicerae and chelifores of crown-group euarthropods and 'great appendages' of other stem lineage deuteropods (summary in Ortega-Hernández et al., 2017). A protocerebral nature of the radiodont frontal appendage (Budd, 2002) has been supported by the highly anterior (preocular) position of these appendages in many radiodont taxa (Ortega-Hernández et al., 2017), developmental data suggesting a paired appendicular nature for the euarthropod labrum (summary in Ortega-Hernández et al., 2017; Budd, 2021), and the neuroanatomy of the radiodont *Lyrarapax* (Figure 1F) (Cong et al., 2014). In contrast, a deutocerebral nature of the radiodont frontal appendage has been suggested largely based on a supposed continuity in frontal appendage morphology between radiodonts and euarthropods (Chen et al., 2004; Haug et al., 2012; Aria and Caron, 2015; Aria et al., 2020; Zeng et al., 2020) and the neuroanatomy of the radiodont *Stanleycaris* (Moysiuk and Caron, 2022). The protocerebral

hypothesis has been contested based largely on redescriptions and reanalyses of the *Lyrarapax* brain anatomy (Aria et al., 2020; Moysiuk and Caron, 2022) and disagreements about the onychophoran anatomy to which *Lyrarapax* is compared (Mayer et al., 2014), whereas the anatomical similarity between radiodont and euarthropod appendages in the deutocerebral hypothesis has alternatively been attributed to convergent evolution based on the similar raptorial predatory feeding mode in these taxa (Ortega-Hernández et al., 2017). No resolution to this debate has yet been provided by the radiodont fossil record.

Nervous system features of the head were first described for *L. unguispinus* (Figure 1F) from the Chengjiang Biota in China (Cong et al., 2014). A single specimen shows carbon-rich regions of darker coloured material that are interpreted to be a protocerebrum with ganglia innervating the frontal appendages situated anterior to the optic tracts linking the eyes to the protocerebral lobes. The protocerebrum is divided into a medial protocerebral neuropil, and a pair of lateral protocerebral lobes. The frontal appendage ganglia are preserved as a pair of almond-shaped pre-ocular domains situated above the base of the frontal appendages, anterior to the medial protocerebral neuropil. The optic nerves show evidence of having two optic neuropils, one distal within the eyecup and one more proximal towards the protocerebrum. The authors describe the frontal appendages as having a pre-protocerebral segmental origin, belonging to an apical segmental unit that was ancestrally separate from the protocerebrum (Strausfeld, 2012), although the presence of such a pre-protocerebral segments within Panarthropoda is unclear (Mayer et al., 2014). If not pre-protocerebral, then the frontal appendages are at least protocerebral in nature (Ortega-Hernández et al., 2017). This brain organisation was described as comparable to that of Onychophora, but not of Eurarthropoda. Any morphological similarity between the frontal appendages of Radiodonta and the 'great appendages' of Deuteropoda, or the chelicera and antennae of crown group Euarthropoda, were therefore concluded to be the result of convergent evolution (Cong et al., 2014).

The neuroanatomy of *Lyrarapax* as presented by Cong et al. (2014) has been contested by Moysiuk and Caron (2022), based on new anatomical data described for the Burgess Shale radiodont *S. hirpex* (Moysiuk and Caron, 2022). In this taxon, multiple specimens preserved traces in the head that are rich in carbon, aluminum and potassium, interpreted as neuroanatomy. In *Stanleycaris*, the most anterior structures connected to the brain with visible nervous tissues are the lateral eyes, with well-preserved optic nerves consisting of a relatively large first optic neuropil that occupied much of the interior of the eye, followed by a more proximal globular neuropil that was smaller in size and located in the eye stalk (Moysiuk and Caron, 2022). Thick optic nerves connect this proximal neuropil to a supraoral neural mass, which consists of a black band crossing the midline between the lateral eyes with circumesophageal connectives that straddle the foregut and are connected posteroventrally to it by a commissure. As described above, a median eye has also been suggested to be present in *Stanleycaris*, with innervation to the supraoral neural mass (Moysiuk and Caron, 2022). Nerves are also seen extending from the brain into the frontal appendages, which are situated ventral relative to the eyes. Altogether, this neural mass is the brain, which the authors describe as being a highly integrated combination of the protocerebrum, to which the median and lateral eye neuropils connect, and the thick circumesophageal connectives being the deutocerebrum, which innervated the frontal appendage (Moysiuk and Caron, 2022). The bipartite brain in *Stanleycaris* shows no evidence of a tritocerebrum.

Based on their description of the neuroanatomy in *Stanleycaris,* Moysiuk and Caron (2022) reinterpret the structures in *Lyrarapax* identified as the frontal appendage ganglia to instead be the median eye neuropil. Their description of the innervation of the head of both *Stanleycaris* and *Lyrarapax* is that the eyes have the most anterior innervation to the brain, with the frontal appendage nerves innervating to the brain proximal and ventral to the optic nerves, with those frontal appendage nerves sometimes projecting anterior to the optic nerves when viewed dorsally. They conclude that the frontal appendage must be innervating the deutocerebrum based on the position of elements in the head, but this innervation is not directly observed in the fossils. The evolutionary scenario they present is that of homology between the radiodont and euarthropod frontal appendages, rejecting the hypothesis supported by the original interpretation of *Lyrarapax* having a protocerebral frontal appendage (Moysiuk and Caron, 2022). The debate about the nature of the brain innervation of the frontal appendages of Radiodonta remains open.

The nervous system of the body trunk in Radiodonta is relatively poorly known, with only rare specimens of *Stanleycaris* preserving it (Moysiuk and Caron, 2022). A pair of thin dark linear features running down the body trunk axis may represent a pair of ventral nerve cords, and no evidence of segmentally arranged ganglia were observed. The authors take this as evidence that an integrated protocerebrum and deutocerebrum evolved first, before the ganglianation of the nerve cord in the body.

4 Diversity and systematics of Radiodonta

At the time of publication, there are 37 species and 25 genera (without any separation of "*Anomalocaris*" and not including *Parapeytoia*) of radiodonts described, or at least radiodont relatives (Supplementary Datasheet S1 and Supplementary Table S2). They are divided into 4 families, the Amplectobeluidae, the Anomalocarididae, the Hurdiidae and the Tamisiocarididae (Lerosey-Aubril and Pates, 2018). Some species are placed into an *Incertae sedis* section because of the difficulty in placing them into a family.

4.1 Amplectobeluidae

Taxa included: *Amplectobelua stephenensis* (Daley and Budd, 2010), *A. symbrachiata* (Hou et al., 1995), *Guanshancaris kunmingensis* (Wang et al., 2013), *Lyrarapax trilobus* (Cong et al., 2016), *L. unguispinus* (Cong et al., 2014), *Ramskoeldia consimilis* (Cong et al., 2018), *R. platyacantha* (Cong et al., 2018). The formal diagnosis of Amplectobeluidae appears in Pates et al. (2021a), following two previous invalid attempts by Vinther et al. (2014) and Cong et al. (2018).

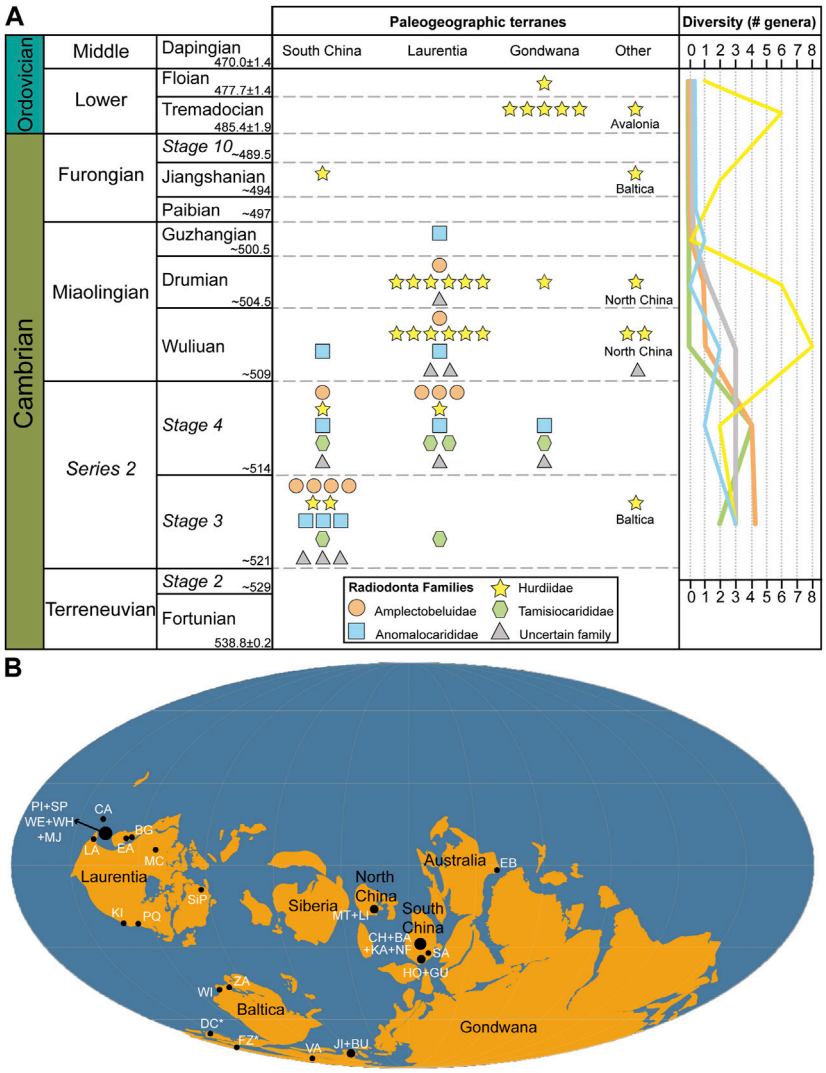

FIGURE 7
Radiodont distribution. **(A)** Stratigraphic distribution during the Cambrian and Lower Orodovician. Each symbol indicates one genus belonging to one the four Radiodonta families and those of uncertain affinity, with paleogeographic terranes represented in vertical columns. For example, in Series 2 Stage 3 of South China, described radiodonts include three Anomalocarididae genera, four Amplectobeluidae genera, two Hurdiidae genera, one Tamisiocaridiidae genus and four genera of uncertain family affiliation. Total number of genera found in each geological time period (for all paleogeographic regions combined) indicated in the line graph on the right. **(B)** Paleogeographic distribution of Lagerstätten that have yielded radiodonts. Abbreviations: (Laurentia) PI, Pioche Fm.; SP, Spence Shale; WE, Weeks Fm.; WH, Wheeler Fm.; MJ, Marjum Fm.; CA, Carrara Fm.; LA, Latham Shale; EA, Eager Fm.; BG, Burgess Shale; KI, Kinzers Fm.; SiP, Sirius Passet; PQ, Parker Quarry; (North China) MT, Mantou Fm.; LI, Linyi Fm.; (South China) CH, Chengjiang Biota; BA, Balang Fm.; KA, Kaili Fm.; SA, Sandu Fm.; HO, Hongjingshao Fm.; GU, Guanshan Biota; NF, Niutitang Formation (Australia) EB, Emu Bay Shale; (Baltica) ZA, Zawiszyn Fm.; WI, Wisniowka Fm.; (Gondwana) JI, Jince Fm.; BU, Buchava Fm.; VA, Valdemiedes Fm.; FZ, Fezouata Shale; (Avalonia) DC, Dol-cyn Afon Gam; *, Ordovician. Map from (Torsvik and Cocks, 2017) gplates package.

This family includes 7 species that has been discovered in 9 localities (Chengjiang Biota, Guanshan Biota, Niutitang Formation, Fandian Biota, Parker Quarry, Kinzers Shale, Latham Shale, Burgess Shale and the Wheeler Formation), corresponding to the paleocontinents of Laurentia and South China, and confined to equatorial and tropical low paleolatitudes (Hou et al., 1995; Steiner et al., 2005; Daley and Budd, 2010; Wang et al., 2013; Cong et al., 2014; Cong et al., 2016; Cong et al., 2017; Cong et al., 2018; Liu et al., 2018; Zeng et al., 2018; Pates and Daley, 2019; Du et al., 2020; Lerosey-Aubril et al., 2020; Pates et al., 2021a; Jiao et al., 2021; Pari et al., 2021; Pari et al., 2022). The first amplectobeluids appeared during Cambrian Stage 3 in South China, and the last representative dates from the Drumian in Laurentia (Hou et al., 1995; Daley and Budd, 2010; Wang et al., 2013; Cong et al., 2014; Cong et al., 2016; Cong et al., 2017; Cong et al., 2018; Liu et al., 2018; Lerosey-Aubril et al., 2020).

In the Chengjiang Biota (Cambrian Stage 3—South China) the oldest known Amplectobeluidae are also the most diverse with *A. symbrachiata* (Figure 4G), *R. platyacantha* (Figure 4H), *R. consimilis*, *L. trilobus* and *L. unguispinus* (Figure 1F) (Hou et al., 1995; Cong et al., 2014; Cong et al., 2016; Cong et al., 2017; Cong et al., 2018; Liu et al., 2018). A possible Amplectobeluidae also occurs

in the Fandian Biota (Cambrian Stage 3—South China) (Du et al., 2020). *Amplectobelua symbrachiata* has been described from the Niutitang Formation (Cambrian Stage 3—South China) (Steiner et al., 2005). The Guanshan Biota (Cambrian Stage 4—South China) is the only locality in which we find *Guanshancaris kunmingensis* (previously called "*Anomalocaris*" *kunmingensis*) (Wang et al., 2013; Zeng et al., 2018; Jiao et al., 2021; Zhang et al., 2023). The Latham Shale, also Stage 4 (Laurentia), has yielded *Ramskoeldia* cf. *consimilis* (Briggs and Mount, 1982; Pates et al., 2021a), and the Kinzers Formation (Cambrian Stage 4—Laurentia) yields a specimen identified as *Amplectobelua* aff. *symbrachiata* (Pates and Daley, 2019). A possible Amplectobeluidae has been described from the Parker Quarry (Cambrian Stage 4—Laurentia) (Pari et al., 2021; Pari et al., 2022). In the emblematic Burgess Shale (Wuliuan - Laurentia), there is *A. stephenensis* (Daley and Budd, 2010). The youngest amplectobeluids are from the Wheeler Formation (Drumian—Laurentia) with *Amplectobelua* cf. *A. stephenensis* (Lerosey-Aubril et al., 2020).

Morphologically speaking, the family is characterized by the presence of gnathobase-like structures (GLSs) and associated smooth and tuberculate plates that were not arranged in a radial oral cone (Figures 3G,H), as well as by aspects of the frontal appendage. The GLSs were roughly rectangular at the base, and bear at least two rows of curved, stout distal spines in sockets at the distal side. The posterior region of the head is characterised by reduced transitional segments. The frontal appendage consists of three podomeres in the proximal region, and in the intermediate region there is an enlarged endite on the fourth podomere, which could in some genera be hypertrophied. The rest of the intermediate and distal podomeres of the frontal appendage bear paired endites that are generally shorter than the height of the podomere to which they attach. These endites decrease in size distally, except for that on podomere 8, which is larger than the endite of podomere 6. The pair of endites on these podomeres can be asymmetrical, consisting of one large endite in typical ventral orientation and a second smaller spinous endite oriented laterally and perpendicular to the larger endite, as seen in *Ramskoeldia* (Figure 1H) and *Amplectobelua* (Figures 3F, 4G) (Cong et al., 2017; Cong et al., 2018). This asymmetry has the potential to cause taxonomic confusion in specimen identification, because the apparent size and/or length of endites can vary depending on the angle of preservation of the appendage relative to the sediment surface (Cong et al., 2018). This is particularly important for distinguishing Amplectobeluidae appendages from those of Anomalocarididae, which can be quite similar in general aspect, but are distinguished by the enlarged endite of the fourth podomere and the endites of podomere eight being larger than those of podomere 6 in Amplectobeluidae. Both of these features are diagnostically absent in Anomalocarididae appendages, but could easily be subjet to taphonomic alteration in some specimens. Taphonomy must be considered when making interpretations about about endite anatomy, especially in isolated specimens, as smaller structures such as asymmetrical endites and auxiliary spines can often be missing or distorted.

The cephalic carapaces of amplectobeluids consist of a relatively small central element, and two oval lateral carapace elements of roughly similar size to the central carapaces. The body of amplectobeluids is characterised by having a relatively small head and well-developed wide flaps, and well as furca in the tail region, based on the whole-body specimens known only for *A. symbrachiata* (Chen et al., 1994) and *L. unguispinus* (Cong et al., 2014; Cong et al., 2016).

4.2 Anomalocarididae

Taxa included: *Anomalocaris canadensis* (Whiteaves, 1892), *Lenisicaris pennsylvanica* (Resser, 1929), *Lenisicaris lupata* (Wu et al., 2021b).

With only 3 formally described species in 2 genera, Anomalocarididae was the first radiodont family discovered but it is the least diverse (Raymond, 1935; Wu et al., 2021b). Its membership is generally not well resolved (see Section 5 below). Representatives of this family are found in 9 localities (Yu'anshan Fm., Hongjingshao Fm., Eager Fm., Emu Bay Shale, Balang Fm., Kinzers Fm. Kaili Fm., Burgess Shale and Weeks Fm.), from the Cambrian Stage 3 to the Guzhangian and belonging to three paleogeographical domains (Laurentia, South China and Australia) between the latitudes of 0°–30°, so limited to only the equatorial and tropical regions (Wu et al., 2021b).

Only three species have been formally described, but Anomalocarididae could include at least 12 more morphologies, with six of them identified as unnamed *Anomalocaris* sp. (Wu et al., 2021b). The Chengjiang Biota yields the first anomalocaridids, including *L. lupata*, *Anomalocaris* cf. *canadensis*, and at least two unnamed *Anomalocaris* sp. (Hou et al., 1995; Wu et al., 2021b). In the Cambrian Stage 3 of the Fandian Biota, an Anomalocarididae has been found but left in open nomenclature (Du et al., 2020). Another Stage 3 site yielding Anomalocarididae is the Hongjingshao Formation, also from South China, with an *Anomalocaris* sp. only (Zhang et al., 2001; Luo et al., 2008; Wu et al., 2021b). The Eager Formation (Cranbrook Shale) (Stage 4, Laurentia) has yielded the oldest known *Anomalocaris canadensis* appendages (Figure 4F) (Briggs, 1979; Whittington and Briggs, 1985; Wu et al., 2021b). The Emu Bay Shale, (Stage 4), the only Australian (Gondwana) locality has also yielded an *Anomalocaris* cf. *canadensis* (Paterson et al., 2011; Daley et al., 2013b; Wu et al., 2021b). Another South China locality, the Balang Formation (Stage 4) has also yielded another *Anomalocaris* sp. (Liu, 2013; Wu et al., 2021b). The last Stage 4 locality is the Kinzers Formation, (Laurentia), from which *L. pennsylvanica* is known (Briggs, 1979; Pates and Daley, 2019; Wu et al., 2021b). The Kaili Formation (Wuliuan) is the first formation from the Miaolingian and the youngest locality from the South China domain that has Anomalocarididae, with another species of *Anomalocaris* sp. (Zhao et al., 2005; Zhao et al., 2011; Wu et al., 2021b). Another major Wuliuan locality with Anomalocarididae is the famous Burgess Shale (Laurentia), which has yielded the emblematic apex predator *Anomalocaris canadensis*, the first ever described radiodont (Whiteaves, 1892; Briggs, 1979; Whittington and Briggs, 1985; Daley and Edgecombe, 2014; Wu et al., 2021b). It is in the Weeks Formation (Cambrian - Miaolingian - Guzhanshian, Laurentia) that the youngest representatives of Anomalocarididae have been found, consisting of *Anomalocaris* aff. *canadensis* and an *Anomalocaris* sp. (Lerosey-Aubril et al., 2014; Wu et al., 2021b).

Anomalocarididae are similar to Amplectobeluidae in having relatively small heads with diminutive cephalic carapaces, but large well-developed flaps and tail furca. Anomalocarididae can be

distinguished from Amplectobeluidae by their frontal appendages, which bear symmetrical paired endites and lack the enlarged endite on podomere 4, and which do not show larger endites on podomere 8 as compared to podomere 6. The oral cone of Anomalocarididae also has a distinct morphology. This structure is known only from *Anomalocaris canadensis* (Figures 1C, 3I, 4F), and it has a unique symmetry among radiodont oral cones because it is triradial (Figure 3I), which means that there are only three large plates that overlap the others. Most other radiodont oral cones have tetraradial symmetry with four large plates (Daley and Bergström, 2012). However, it is not known if this triradial oral cone is a common character for the entire Anomalocarididae family, because *Lenisicaris* is known only from frontal appendages so far (Resser, 1929; Pates and Daley, 2019; Wu et al., 2021b).

4.3 Hurdiidae

Taxa included: *Aegirocassis benmoulai* (Figures 1E, 4D,E) (Van Roy et al., 2015), *Buccaspinea cooperi* (Figure 3D) (Pates et al., 2021b), *Cambroraster falcatus* (Moysiuk and Caron, 2019), *Cordaticaris striatus* (Figure 3J) (Sun et al., 2020a), *Hurdia victoria* (Figures 4A; 6A–C,E) (Walcott, 1912), *Hurdia triangulata* (Figures 1B, 6D) (Walcott, 1912), *Pahvantia hastata* (Robison and Richards, 1981), *Peytoia infercambriensis* (Lendzion, 1975), *Peytoia nathorsti* (Figures 1D, 3A–C, 4B) (Walcott, 1911), *Stanleycaris hirpex* (Figure 4C) (Caron et al., 2010), *Titanokorys gainesi* (Caron and Moysiuk, 2021), *Ursulinacaris grallae* (Pates et al., 2019). The diagnosis written for the Hurdiidae family by Lerosey-Aubril and Pates (2018) was revised by Wu et al. (2022) and Moysiuk and Caron (2022).

Questionably: *Pseudoangustidontus duplospineus* (Van Roy and Tetlie, 2006), *Schinderhannes bartelsi* (Kühl et al., 2009).

Informally called hurdiids, this family is the most diverse and best resolved (Figure 8) among the radiodonts, with 12 species described in 10 genera. Moreover, two other species (two genera) could questionably belong to Hurdiidae. It is also the family that has the longest history, with fossils found from the Cambrian Stage 3 to the Lower Ordovician, and possibly the Devonian (Van Roy and Tetlie, 2006; Kühl et al., 2009; Van Roy et al., 2015; Wu et al., 2022). They have been found in 19 localities (20 if the Wheeler Formation is divided in two as suggested in Wu et al., 2022), with 16 of those being from the Cambrian, corresponding to five palaeogeographical domains and two localities from one domain during the Ordovician (Wu et al., 2022). The stratigraphically oldest fossil of any known radiodont is the hurdiid *Peytoia* from the Zawiszyn Formation (Baltica) of Cambrian Stage 3 (Daley and Legg, 2015; Wu et al., 2022). In the slightly younger Chengjiang Biota, *Cambroraster* and a Hurdiidae indet have been described. In the Balang Formation (Cambrian Stage 4 - South China), another *Peytoia* has been described (Liu, 2013; Wu et al., 2022). The last Series 2 hurdiid is *Hurdia* found in the Pioche Formation in the Ruin Wash *lagerstätte* (Stage 4 - Laurentia) (Pates et al., 2021a; Wu et al., 2022). In the Carrara Formation and in the Mount Cap Formation (Wuliuan - Laurentia), the only hurdiid found is *Ursulinacaris* (Pates et al., 2019; Wu et al., 2022). Then, in the Spence Shale (Wuliuan - Laurentia), two hudiid taxa are reported, *Buccaspinea* and *Hurdia* (Daley et al., 2013a; Pates et al., 2021a; Wu et al., 2022). The Burgess Shale (Wuliuan - Laurentia) contains an abundant hurdiid assemblage, including *Cambroraster*, *Hurdia* (Figures 1B, 3E, 4A, 6A–E), *Peytoia* (Figures 1D, 3A–C, 4B), *Stanleycaris* (Figure 4C) and *Titanokorys* (Whittington and Briggs, 1985; Collins, 1996; Caron et al., 2010; Daley et al., 2013a; Moysiuk and Caron, 2019; Caron and Moysiuk, 2021; Moysiuk and Caron, 2021; Moysiuk and Caron, 2022; Wu et al., 2022). The last Wuliuan locality with hurdiid specimens is the Mantou Formation (North China) with *Cambroraster* and another hurdiid indet (Sun et al., 2020b; Wu et al., 2022). The Wheeler Formation (Drumian - Laurentia) has yielded five taxa, *Buccaspinea*, *Hurdia*, *Pahvantia*, *Peytoia* and *Stanleycaris* (Robison and Richards, 1981; Pates et al., 2017; Pates et al., 2018; Pates et al., 2021b; Wu et al., 2022). The Wheeler Formation and the Burgess Shale are the localities with the highest generic diversity of hurdiids (Wu et al., 2022). The second and last North China locality is the Zhangxia Formation (Drumian), in which the only hurdiid found is *Cordaticaris* (Sun et al., 2020a; Sun et al., 2022; Wu et al., 2022). The last Laurentia site with hurdiids, also from the Drumian, is the Marjum Formation, in which have been found three hurdiid taxa, *Buccaspinea* (Figure 3D), *Pahvantia* and *Peytoia* (Pates et al., 2021a; Pates et al., 2021b; Wu et al., 2022). The last Drumian localities are the Jince Formation and the Buchava Formation (Czech, Gondwana) with *Hurdia* (Chlupáč and Kordule, 2002; Mikuláš et al., 2012; Daley et al., 2013a; Wu et al., 2022). The only two hurdiids found in the Furongian, and the last of the Cambrian hurdiids, are from the Sandu Formation (Jiangshanian—South China) with an undetermined hurdiid and the Wiśniówka Formation (Jiangshanian—Baltica) with a *Peytoia* (Zhu et al., 2021; Wu et al., 2022). In the Ordovician, there is the Afon Gam (Tremadocian—Avalonia) that has a hurdiid specimen (Pates et al., 2020; Wu et al., 2022). The stratigraphically youngest formally described hurdiid is *A. benmoulai* (Figures 3E, 4D,E), from the Fezouata Shale (Tremadocian—Morocco, Gondwana) (Van Roy and Briggs, 2011; Van Roy et al., 2015; Wu et al., 2022). The Tremadocian Fezouata Shale also has yielded an undertermined hurdiid (Van Roy and Briggs, 2011; Wu et al., 2022). However, in the Floian Fezouata Shale, the enigmatic *Pseudoangustidontus* or a large carapace of possibly radiodont affinity could be even younger hurdiids (Van Roy and Tetlie, 2006). The highly debated *Schinderhannes* from the Esmian Kaub Formation (Devonian—Germany, Laurussia) has been suggested by some authors to be a hurdiid (Van Roy and Tetlie, 2006; Kühl et al., 2009; Van Roy et al., 2015; Saleh et al., 2022b; Wu et al., 2022), although restudy of the material is needed to confirm this.

Hurdiid morphology is characterized by the form of the frontal appendage, oral cone and cephalic carapaces (Figures 1B,D,E, 3A–E, 4A–E, 6A–E). Unique to this family are frontal appendages with elongated ventral endites that are usually blade-like and bearing auxiliary spines along one margin only (Lerosey-Aubril and Pates, 2018; Moysiuk and Caron, 2022; Wu et al., 2022). Within hurdiids, the podomeres are divided in 3 categories (Lerosey-Aubril and Pates, 2018; Wu et al., 2022). The proximal region has one or more podomeres, to which a short endite may be attached (Lerosey-Aubril and Pates, 2018; Wu et al., 2022). The intermediate podomeres bear one laminiform endite each in most (or all) taxa, which are at least two times longer than the height of the podomere to which they attach, but can be more than eight times longer in

Aegirocassis (Van Roy et al., 2015; Lerosey-Aubril and Pates, 2018). Paired endites have been described only for the hurdiid *U. grallae*, with the five intermediate podomeres bearing two elongated and slender endites each (Pates et al., 2019), although a reinterpretation of this material by Moysiuk and Caron (2021) suggests instead that these are not paired endites, but rather represent the preservation of overlap of the tapered margins of adjacent single laminiform endites, which give the appearance of being two distinct endites. Usually, the intermediate endites number five, but there can be up to eight endites in *Cordaticaris* (Lerosey-Aubril and Pates, 2018; Sun et al., 2020a). In all taxa, they bear auxiliary spines on one side of the endite only. The distal podomeres are reduced in size (length, height or both) compared to the intermediate region, and they can bear short endites in some taxa (Lerosey-Aubril and Pates, 2018), as well as terminal spines (Pates et al., 2019). The intermediate and distal podomeres are together referred to as the distal articulated region in some studies (Supplementary Table S1B), and these podomeres can bear dorsal spines (Pates et al., 2017; Lerosey-Aubril and Pates, 2018; Zeng et al., 2018). Medial spines, referred to a gnathites (Moysiuk and Caron, 2021), are also seen in some Hurdiidae taxa, including *Stanleycaris* (Moysiuk and Caron, 2021), *Peytoia* (Daley et al., 2013a), cf. *Peytoia* (Daley and Budd, 2010) and possibly *Schinderhannes* (Kühl et al., 2009; Moysiuk and Caron, 2021). These relatively large and robust spines are considered to be homologous with one of the paired endites seen in non-hurdiid radiodonts, which has migrated medially and adopted a different function as a masticatory jaw structure (Moysiuk and Caron, 2021). In this respect, the smaller medially-oriented endite of the asymmetrical endite pair seen on each podomere of the Amplectobeluidae frontal appendage could be a transitional character state between the pared symmetrical endites seen on each podomere of Anomalocarididae frontal appendages and the podomeres of Hurdiidae frontal appendages, which bear a single elongated ventral endite and a robust medial endite.

The shape of the oral cone consists of the "classic" tetraradial symmetry with four larger plates arranged in 90° on top of 28 smaller ones (Figures 3A–E) (Daley and Bergström, 2012; Daley et al., 2013a; Lerosey-Aubril and Pates, 2018). However, this oral cone organisation is not unique to Hurdiidae, as it is also seen in *Lyrarapax* and *G. kunmingensis* (Amplectobeluidae) (Lerosey-Aubril and Pates, 2018; Liu et al., 2018; Zeng et al., 2018; Zhang et al., 2023). Another notable feature of the hurdiids is the enlarged cephalic carapace complex, which typically consists of a central element and two lateral elements, and which together can sometimes represent up to half of the total body length, as seen in *Hurdia* (Daley et al., 2009; Daley et al., 2013a). Cephalic carapaces are also observed in other families, however they tend to be smaller than those seen in hurdiids.

4.4 Tamisiocarididae

Taxa included: *"Anomalocaris" briggsi* (Figure 5C) (Nedin, 1995), *Houcaris saron* (Figure 5D) (Hou et al., 1995), *Houcaris magnabasis* (Figure 5B) (Pates et al., 2021a), *Tamisiocaris borealis* (Figure 5A) (Daley and Peel, 2010). The diagnosis of Hurdiidae established in Pates and Daley (2019) was recently revised in Wu et al. (2021a).

With four species, Tamisiocarididae, originally called Cetiocaridae in Vinther et al. (2014), has been found in only seven localities (Emu Bay Shale, Pioche Fm., Chengjiang, Carrara Fm., Kinzers Fm., Guanshan Biota, and Sirius Passet), belonging to three main paleogeography domains (Laurentia, South China and Australia/Gondwana) (Daley et al., 2013b; Paterson et al., 2020; Pates et al., 2021a; Wu et al., 2021a; Jiao et al., 2021). They are from tropical areas only, from the low latitudes between 0° and 30° (Wu et al., 2021a).

Tamisiocaridids are exclusively from Series 2 of the Cambrian (Wu et al., 2021a). The oldest representative is *H. saron* (Figure 5D) from the Chengjiang biota (Stage 3 South China) (Hou et al., 1995; Wu et al., 2021a). *Tamisiocaris borealis* (Figure 5A), also from Stage 3, has been found in the Sirius Passet (Laurentia) (Daley and Peel, 2010; Vinther et al., 2014; Wu et al., 2021a). A Tamisiocarididae indet. has been found in slightly younger strata of the South China domain, in the Guanshan Biota (Stage 4—South China) (Wu et al., 2021a; Jiao et al., 2021). *Tamisiocaris* aff. *borealis* has also been found in the Kinzers Formation (Stage 4—Laurentia) (Pates and Daley, 2019; Wu et al., 2021a). In the Emu Bay Shale, Australia domain (Stage 4—Gondwana), we see "*Anomalocaris*" *briggsi* (Figure 5C) (Daley et al., 2013b; Wu et al., 2022). Finally, the last one is *H. magnabasis* from the Carrara and Pioche (Figure 5B) Formations, both in Laurentia domain and from Stage 4 (Pates et al., 2021a; Wu et al., 2022).

The morphological distinction of Tamisiocarididae is made based on the frontal appendages. The endites are in pairs, and they are very thin and much longer than the height of the podomeres to which they attach (Wu et al., 2021a). The endites from the proximal and intermediate regions all have auxiliary structures (spines or setae) (Wu et al., 2021a).

4.5 *Incertae sedis*

Taxa included: *Caryosyntrips camurus* (Pates and Daley, 2017), *Caryosyntrips durus* (Pates and Daley, 2017), *Caryosysntrips serratus* (Daley and Budd, 2010), *Cucumericrus decoratus* (Hou et al., 1995), *Innovatiocaris maotianshanensis* (Figure 1A) (Zeng et al., 2022), "*Innovatiocaris*" *multispiniformis* (Zeng et al., 2022), *Laminacaris chimera* (Guo et al., 2019), *Paranomalocaris multisegmentalis* (Wang et al., 2013), *Paranomalocaris simplex* (Jiao et al., 2021), *Parapeytoia yunnanensis* (Hou et al., 1995).

Incertae sedis radiodont taxa are not resolved consistently into one family in phylogenetic analyses, because of conflicting characters that make them difficult to interpret. As elaborated below, it seems quite likely that *Innovatiocaris*, *Laminacaris*, *Paranomalocaris* and possibly *Cucumericrus* belong within Radiodonta, but the enigmatic taxa *Caryosyntrips* and *Parapeytoia* may fall outside the clade.

Most of these uncertain taxa have been found in the South China domain, and especially in the Chengjiang Biota, with *C. decoratus*, *I. maotianshanensis*, "*Innovatiocaris*" *multispiniformis*, *L. chimera* and *P. yunnanensis* (Hou et al., 1995; Guo et al., 2019; Zeng et al., 2022). *Paranomalocaris multisegmentalis* and *P. simplex* are also from the South China domain, deriving from the Guanshan Biota (Stage 4) (Wang et al., 2013; Jiao et al., 2021). Outside of the South China domain, we only find *Caryosyntrips* (Daley and Budd, 2010;

Pates and Daley, 2017). From Stage 4, a *Caryosyntrips* cf. *camurus* has been found in the Valdemiedes Formation (Gondwana) (Pates and Daley, 2017). In Laurentia during the Wuliuan, we find *C. camurus* in the Spence Shale (Pates and Daley, 2017) and the Burgess Shale, with this last site also yielding *Caryosyntrips serratus* (Daley and Budd, 2010; Pates and Daley, 2017). Finally, in the Drumian of Laurentia, there are *C. camurus* and *C. durus* from the Wheeler Formation (Pates and Daley, 2017).

All the taxa placed here are debated. *Caryosyntrips*, originally described as a radiodont based on isolated frontal appendages (Daley and Budd, 2010), resolved within Radiodonta in the phylogenetic analyses of Lerosey-Aubril and Pates (2018), but just outside the clade in Moysiuk and Caron (2021). In Zeng et al. (2022), *Caryosyntrips* is nested within the upper stem lineage to Euarthropoda. *Caryosyntrips* is known only from isolated appendages, which are wedged-shaped with a constant taper along their entire length, bearing simple paired spines and dense dorsal spines in some species (Pates and Daley, 2017).

The enigmatic *Cucumericrus* is known from two specimens, only one of which can be seen in a published photograph, with the other known only from a drawing. The specimens both show a flap-like structure bearing striations, associated with a weakly segmented appendage that is described as having gnathobases (Hou et al., 1995). This could represent a radiodont ancestral morphology, perhaps describing either the loss of lobopods or the transformation into flaps (Hou et al., 1995; Edgecombe, 2015; Van Roy et al., 2015).

Innovatiocaris is known from a complete whole-body specimen (Figure 1A) that was originally described under the name *Anomalocaris saron* (Chen et al., 1994; Hou et al., 1995; Wu et al., 2021a). The specimen shows similarities to both Anomalocarididae and Amplectobeluidae, with a body bearing well-developed flaps and a frontal appendage bearing paired endites on all podomeres. Its phylogeny position in Zeng et al. (2022) depends on the analysis. In parsimony analyses, it resolves in a sister clade to that consisting of Amplectobeluidae, Anomalocarididae and Tamisiocarididae, together with *L. chimera* and *G. kunmingensis* (previously called "*Anomalocaris*" *kunmingensis*). With Bayesian inference is resolves as a sister taxon to the hurdiids (Zeng et al., 2022).

Both *Laminacaris* and *Paranomalocaris* are known from isolated frontal appendages. *Laminacaris* has originally not been placed in any family (Guo et al., 2019), because it has an overall morphology of an amplectobeluid or an anomalocaridid, but with the presence of a distinctly hurdiid-like laminiform endite. However, the phylogenetic analyses of both Moysiuk and Caron (2021) and Zeng et al. (2022) placed it as closely related to Amplectobeluidae and Anomalocarididae. *Paranomalocaris* is distinct within radiodont as having a high number of podomeres totaling 22, with its short endites bearing at least five pairs of auxiliary spines (Wang et al., 2013). It was considered in Jiao et al. (2021) to be an Anomalocarididae. In phylogenetic analysis, it is indeed strongly affiliated to this family, but not formally included in it (Lerosey-Aubril and Pates, 2018; Moysiuk and Caron, 2021).

Finally, *Parapeytoia*, associated originally to Anomalocarididae (before the name Radiodonta was erected and its families differentiated), has no documented position within the phylogeny (Hou et al., 1995). It is morphology mixes radiodont features, such as a probable oral cone, with megacheiran features such as gnathobases and a short great appendage (Hou et al., 1995; Chen et al., 2004; Aria et al., 2020; Zeng et al., 2020). Some authors have rejected the inclusion of *Parapeytoia* within Radiodonta (Stein, 2010; Legg, 2013; Cong et al., 2014; Van Roy et al., 2015), although a redescription of the material by Budd (2021) led him to conclude that it likely lies close to the radiodonts in a phylogenetic sense, either as sister-taxon to Radiodonta, to Euarthropoda, or to both.

5 Phylogenetic analyses of radiodont relationships

Phylogenetic inference has been an important tool for resolving the affinity of Radiodonta as stem lineage euarthropods, and also for examining their internal relationships. Radiodonts had been variously interpreted as stem lineage arthropods (Dewel and Dewel, 1998; Budd, 2002), crown-group arthropods (Chen et al., 2004; Maas et al., 2004), as a sister group to arthropods in the broad sense (Wills et al., 1998; Hou et al., 2006), or as cycloneuralian worms (Hou et al., 1995) before the phylogenetic analyses of Kühl et al. (2009) and Daley et al. (2009) independently retrieved a position for radiodonts as basal stem lineage euarthropods, sitting between the gilled lobopodians *Kerygmachela* and *Pambdelurion* from Sirius Passet downtree, and a variety of biramous-limb bearing Cambrian euarthropods in the upper stem (Figure 8A). Since these works in 2009, a flurry of research has revealed many new radiodonts, and the ever-expanding morphological diversity of the clade has naturally led to numerous phylogenetic analyses attempting to resolve their interrelationships (Vinther et al., 2014; Lerosey-Aubril and Pates, 2018; Moysiuk and Caron, 2019; Caron and Moysiuk, 2021; Moysiuk and Caron, 2021; Moysiuk and Caron, 2022; Pates et al., 2022; Zeng et al., 2022). The results showed many similarities and differences, depending on the analytical method and the characters used.

The first phylogenetic analysis that established the four radiodont families was by Vinther et al. (2014). Even if Hurdiidae and Tamisiocarididae are monophyletic in their results, Anomalocarididae appears to be paraphyletic (Vinther et al., 2014). It presents Radiodonta as a monophyletic group, excluding *Caryosyntrips serratus* (Vinther et al., 2014). Cong et al. (2014) and Van Roy et al. (2015) corrected errors in the Vinther et al. (2014) character matrix and used it to code in new radiodont taxa, *Lyrarapax* and *Aegirocassis* respectively, retrieving the same general tree arrangement, with a monophyletic Hurdiidae and Tamisiocarididae as sister clades, with both together being sister to an unresolved group of Anomalocarididae and a monophyletic Amplectobeluidae.

In the analysis of Lerosey-Aubril and Pates (2018), which was based on a matrix that had been considerably recoded from the Van Roy et al. (2015) matrix, their phylogeny recovered a trichotomy between *Caryosyntrips*, an otherwise monophyletic Radiodonta, and the rest of the euarthropod upper stem lineage (Figure 8C). Two main polyphyletic groups are defined, one including the Anomalocarididae, Amplectobeluidae and *Paranomalocaris*, and the other consisting of Hurdiidae and Tamisiocaridiae (Lerosey-Aubril and Pates, 2018).

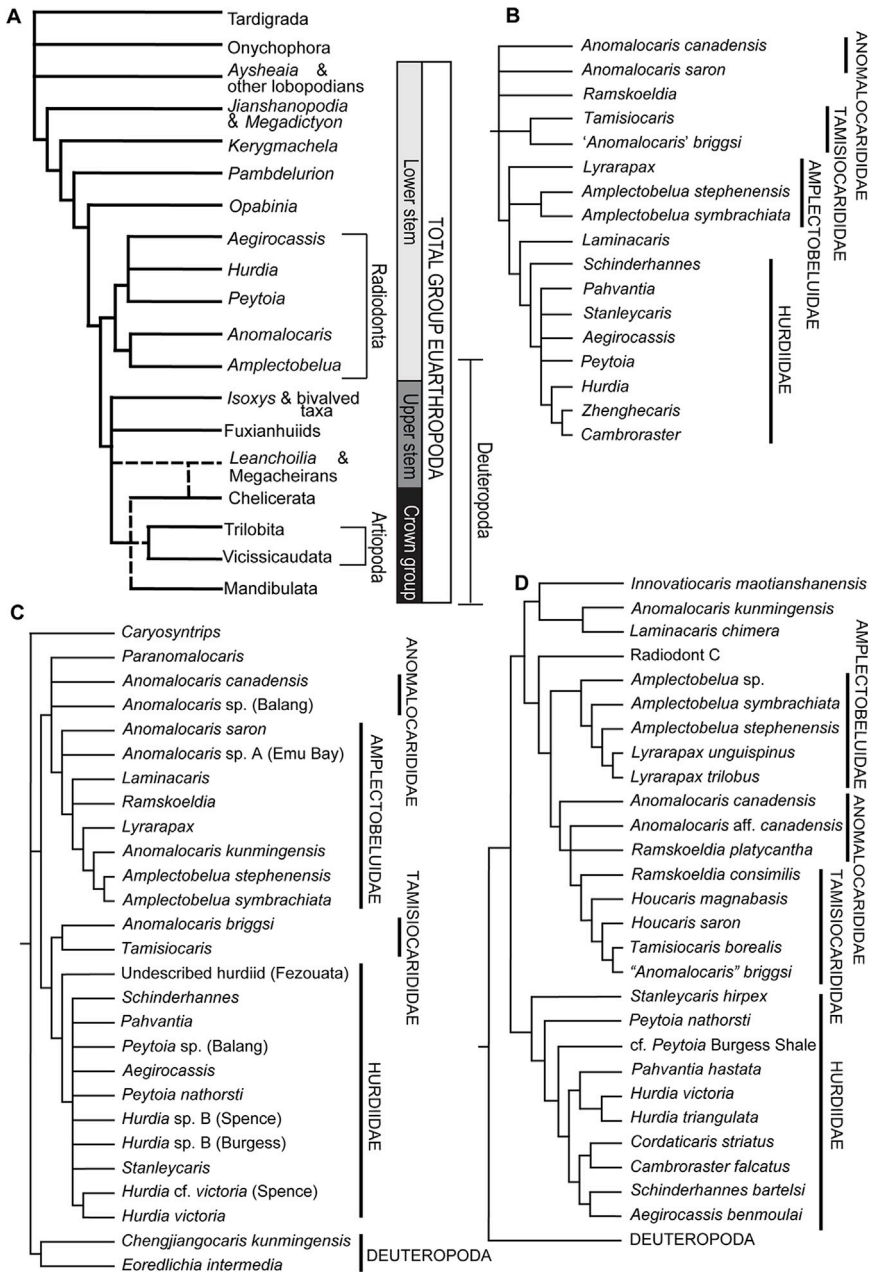

FIGURE 8
Phylogenetic placement of Radiodonta and comparison of the interelationships within the clade. **(A)** A generalised cladogram of euarthropod relationships, showing Radiodonta in the lower stem to Euarthropoda. Megacheira and Artiopoda have uncertain phylogenetic placements, as shown by the dashed lines. Modified from (Daley et al., 2018). **(B)** Radiodonta relationships as retrieved by (Moysiuk and Caron, 2019) using Bayesian majority rule consensus. **(C)** Strict consensus of maximum parsimony tree run under equal weighting by (Lerosey-Aubril and Pates, 2018). **(D)** Maximum parsimony analysis shown with strict consensus from (Zeng et al., 2022).

In the phylogeny of Moysiuk and Caron (2019), *Caryosyntrips* is not considered as a radiodont, and then the order is otherwise monophyletic (Figure 8B). Inside the group, only Hurdiidae and Tamisiocaridiae are monophyletic (Moysiuk and Caron, 2019). It does not retrieve *Ramskoeldia* as belonging to Amplectobeluidae (Moysiuk and Caron, 2019). Amplectobeluidae resolve as the most closely related family to the derived Hurdiidae, with Tamisiocarididae and several unresolved Anomalocarididae taxa being in a basal position within Radiodonta. The phylogenic analyses by these authors continued to evolve with the addition of new radiodonts from the Burgess Shale. Moysiuk and Caron (2021) propose a new phylogeny that was more detailed than their previous attempt. The main difference is that Anomalocarididae and Amplectobeluidae are retrieved as a monophyletic group, in which there is the "Amplectobeluidae *sensu stricto*" with *Amplectobelua* and *Lyrarapax* only (Moysiuk and Caron, 2019). Hurdiidae and Tamisiocarididae still resolve as

monophyletic clades, but are unresolved with respect to each other and to the Anomalocarididae + Amplectobeluidae clade, such that it is unclear which is basal and which is derived. Their next version of the tree (Caron and Moysiuk, 2021) retrieves a basal monophyletic Tamisiocarididae, followed by an unresolved node of the "Amplectobeluidae *sensu stricto*" (name from Moysiuk and Caron, 2021), a monophyletic Hurdiidae, and the paraphyletic mix of *Anomalocaris* and *Laminacaris* species (Caron and Moysiuk, 2021).

The phylogenetic analysis of Pates et al. (2022) had a larger focus on resolving the position of Opabiniidae, which was previously aligned together with Radiodonta in the Class Dinocarida (Collins, 1996). Most phylogenies do not resolve a sister group relationship between Opabiniidae and Radiodonta, with *Opabinia* typically sitting either downtree or uptree from Radiodonta (Figure 8A). In this analysis, Opabiniidae is immediately downtree from a paraphyletic grade of radiodont taxa (Pates et al., 2022). The study generally retrieves a monophyletic clade consisting of Amplectobeluidae, Anomalocarididae and Deuteropoda, separate from a poorly resolved Hurdiidae clade (Pates et al., 2022). In this analysis, relatively few radiodont taxa were included and the authors indicate that the character matrix and model of morphological change are not optimized for resolving the internal relationships of radiodonts, because the focus was on broader relationships within the euarthropod stem lineage.

Zeng et al. (2022) performed a parsimony analysis (Figure 8D) and Bayesian inference, both of which present Radiodonta as a monophyletic group (Zeng et al., 2022). *Caryosyntrips* is retrieved in the upper stem lineage of Euarthropoda (Zeng et al., 2022). The maximum parsimony tree (Fig.15a in Zeng et al., 2022) shows a monophyletic Hurdiidae in sister group relationship to a clade consisting of the rest of the radiodont taxa (Figure 8D). *Laminacaris*, *Guanshancaris* ("*Anomalcoaris*" *kunmingensis*) and *Innovatiocaris* are found basal to all non-hurdiid radiodonts. A monophyletic Tamisiocariidae is derived within a grade of paraphyletic "Anomalocarididae", all of which is in a sister group relationship to Amplectobeluidae. The second tree, a 50% majority-rule consensus from Bayesian inference, is different because the group with *Laminacaris*, *Guanshancaris* and *Innovatiocaris* now paraphyletic (Zeng et al., 2022). *Innovatiocaris* moves to a basal position in the Hurdiidae clade, while the monophyletic clades of Tamisiocarididae and Amplectobeluidae are in an unresolved node with a variety of "Anomalocarididae" taxa.

Some common conclusions can be reached when examining these trees. Radiodonta is usually found to be monophyletic if *Caryosyntrips* is excluded, and the Hurdiidae family is also always monophyletic and generally well resolved. Amplectobeluidae and Anomalocarididae are often found closely associated, but the position of Tamisiocarididae is highly unstable. Anomalocarididae is usually poorly resolved, and much work is needed to revise the membership and phylogenetic relationships of this family. It is unclear which family occupies a basal position within Radiodonta, making it impossible to understand character polarization.

6 Biogeographic and temporal distribution of Radiodonta

Radiodonts colonized almost all the major paleogeographic domains during the Cambrian (Figure 7B), from all latitudes, however the majority occupied the South Hemisphere and were found in equatorial and tropical areas (Wu et al., 2021a; Wu et al., 2021b; Wu et al., 2022). From Siberia, only one enigmatic specimen (Ponomarenko, 2010) of a possible body has been described as a dinocaridid, but we do not find any convincing argument to include it within Radiodonta. During the Ordovician, the biogeographical repartition is restricted to the south high latitude of Avalonia and North Africa (Gondwana) domain (Van Roy et al., 2015; Pates et al., 2020; Wu et al., 2022).

The paleogeographic and temporal repartition is different between the families, even if they have many similarities (Wu et al., 2021a; Wu et al., 2021b; Wu et al., 2022). Generally speaking, Anomalocarididae and Amplectobeluidae in South China are more diverse and abundant early in radiodont history (Series 2 Stage 3), followed by a slight peak in a geographically widespread Tamisiocarididae during Series 2 Stage 4. Series 3 is dominated instead by a diverse and abundant Hurdiidae, especially in Laurentia but with occurrences in all paleogreographic domains, that persists as the only radiodont family found after the Miaolingian (Figure 7A).

Focusing on paleogeography, we see that at first, during the Cambrian, the majority of taxa in all families are found in South China and Laurentia paleocontinents, especially with Chengjiang, Burgess Shale and the Great Basin *lagerstätten* (Wu et al., 2021a; Wu et al., 2021b; Wu et al., 2022). Most of the species are found in the equatorial and tropical latitude, between 0° and 30°. All families (Amplectobeluidae, Anomalocarididae, Hurdiidae and Tamisiocarididae) occupied Laurentia and South China, and in Australia (Gondwana) there were only Tamisiocarididae and Anomalocarididae (Supplementary Table S2). Amplectobeluidae, Anomalocarididae and Tamisiocarididae lived at exclusively equatorial and tropical latitudes (Figure 7; Supplementary Table S2). Hurdiidae are the most geographically widespread, being the only family found in the North China domain so far (Sun et al., 2020a; Wu et al., 2022). It is also the only family that lived in higher latitudes, in Baltica at a bit more than 30°, and in Czech at around 60°, during the Cambrian (Chlupáč and Kordule, 2002; Mikuláš et al., 2012; Zhu et al., 2021; Wu et al., 2022). During the Lower Ordovician, there were only hurdiids found, with fossils collected from high paleolatitudes of the southern hemisphere under the 60°S latitude in the north margin of Gondwana and the south of Avalonia, both surrounding the Rheic ocean that was opening at that time (Van Roy et al., 2015; Pates et al., 2020; Zhu et al., 2021; Wu et al., 2022). The problem of the Lower Ordovician is that *lagerstätten* are rare, and only two have yielded described radiodonts (Van Roy et al., 2015; Pates et al., 2020; Zhu et al., 2021; Wu et al., 2022).

The temporal distribution is not uniform either, although a lot of variation appears to be dependent on the irregular distribution of *lagerstätten* in time (Wu et al., 2021a; Wu et al., 2021b; Wu et al., 2022). The oldest known radiodont is the *Peytoia infercambriensis* (Hurdiidae) from the Zawiszyn Formation in Poland, that is dated from the Cambrian Series 2 Stage 3 (Daley and Legg, 2015; Wu et al., 2022). Radiodonts were most abundant and diverse during Cambrian Series 2 and the Miaolingian, but it is only during Series 2 that we find all four families, because Tamisiocarididae are exclusively known from this time period (Supplementary Table S2). Series 2 is also the peak of diversity for Amplectobeluidae and Anomalocarididae,

well documented by the Chengjiang Biota (Supplementary Table S2). During the Miaolingian, Amplectobeluidae and Anomalocarididae have a decrease in diversity, while the Hurdiidae have an increase in the Wuliuan and the Drumian, with the Burgess Shale and the Wheeler Formation, for example, (Figure 7). Then, in the Guzhangian, there were only Anomalocarididae specimens from the Weeks Formation (Lerosey-Aubril et al., 2014; Wu et al., 2021b). During the Furongian, a gap in *lagerstätten* is seen, and only two hurdiid radiodonts occur in the Jiangshanian Sandu and Wiśniówka Formations (Harper et al., 2019; Zhu et al., 2021). In the Lower Ordovician, there is another hurdiid in the Dol-cyn Afon-Gam of Wales (Pates et al., 2020). The youngest radiodont is debated. It could be *A. benmoulai*, from the Tremadocian Fezouata Shale (Morocco), that is formally described as an hurdiid radiodont (Van Roy et al., 2015; Wu et al., 2022). Otherwise, there are two other possible candidates but their membership within Radiodonta is under debate. *Pseudoangustidontus duplospineus* from the Floian Fezouata Shale (Morocco), or *Schinderhannes bartelsi* from the Emsian (Lower Devonian) Hunsrück Slate of the Kaub Formation (Germany) (Van Roy and Tetlie, 2006; Kühl et al., 2009; Wu et al., 2022), both of which are problematic, for reasons discussed earlier. If *S. bartelsi* is a radiodont, a huge gap would exist between the Lower Ordovician and the Lower Devonian (Kühl et al., 2009; Van Roy et al., 2015; Wu et al., 2022).

7 Conclusion: Significance of Radiodonta for understanding paleoecology and evolution during the early Paleozoic

As summarized above, Radiodonta represent a diverse and abundant group that was globally distributed during the Cambrian and Lower Ordovician. Despite having been first discovered over 130 years ago, their overall body architecture was not accurately reconstructed until nearly 100 years later, and over 90% of their known diversity has been described in the last 15 years. This explosion in recent discoveries has revealed that radiodonts populated all major paleocontinents at a variety of paleolatitudes, showcasing their adaptability and highly mobile lifestyle. As shown in this review, radiodont anatomy has provided important insight into the evolution of several defining features of Euarthropoda, and various functional morphology and quantitative approaches can be used to reconstruct their paleoecology.

Radiodonta undoubtedly had a major impact on the earliest animal ecosystems. Apex consumers in general have long been suggested to have the ability to shape ecosystems, in a trophic cascade the propagates impacts from consumers on the size, abundance, diversity and behaviour of prey taxa that make up food webs (Hairston et al., 1960; Paine, 1980; Fretwell, 1987; Terborgh and Estes, 2010; Estes et al., 2011). This is known as 'top-down control', and in the Cambrian the introduction of metazoan consumers into a plankton ecosystem previously devoid of such organisms accounts for subsequent diversifications and developments of complexity in ecosystems during the Cambrian in general (Butterfield, 2000), with arthropod predators such as the diverse, abundant and globally-distributed radiodonts playing an important role (Budd, 2000; Vannier, 2007). As described above, radiodont morphology indicates their predatory lifestyle, and some localities indicate that multiple taxa lived in close proximity (Caron and Jackson, 2008; Dunne et al., 2008), sometimes found on the same rock sample centimeters apart from each other (Daley and Budd, 2010). Competition between conspecific radiodont predators likely accelerated evolution within the group, and their increased specialization towards different feeding behaviours would have driven evolution of defensive mechanisms in their prey, contributing to an overall arms race that helped shape the complexity of Cambrian and Early Ordovician ecosystems (Marshall, 2006; Bush and Bambach, 2011).

Radiodonts represent some of the earliest animals that colonized the water column, as indicated by their high abundance in numerous globally-distributed Cambrian and early Ordovician lagerstätten, which capture especially those animals that were swimming close to the seafloor (Saleh et al., 2021). In large-scale quantitative analyses of the patterns of nektonization during the Palaeozoic (e.g., Klug et al., 2010; Whalen and Briggs, 2018), radiodonts are classified as belonging to the demersal megaguild, and specifically having a eudemersal ecomorphological life mode (obligate swimmers restricted to near-benthic settings). Such analyses revealed that demersal taxa made up an important proportion of the organisms occupying the water column and accounted for the greatest proportion of diversity from the Terreneuvian through the Miaolingian, with radiodonts being important arthropod contributors to this category (Klug et al., 2010; Whalen and Briggs, 2018). These quantitative studies only considered a portion of radiodont generic diversity, with databases typically including only 6 or 7 genera. Given that this value is now known to be at least 25 radiodont genera (Supplementary Datasheet S1), it stands to reason that they would have made up an even more important proportion of Cambrian eudemersal taxa, and would have contributed to the impact of this life mode on the early evolutionary dynamics of colonization of the water column. Hints about the eventual extinction of radiodonts can also be found when examining the subsequent dominant eudemersal taxa, with nautiloid cephalopods largely replacing radiodonts in the Furongian and through the Ordovician, eventually joined by jawed armoured fishes (arthrodire "placoderms") and ammonoids in the Devonian (Whalen and Briggs, 2018). Radiodonts were presumably less efficient eudemersal predators, and their diversification of suspension feeding coupled with a relatively large body size in the Ordovician may represent both an attempt to avoid direct competition with new predators while also exploiting the rapidly diversifying plankton food source at the start of the Ordovician plankton revolution (Servais et al., 2016).

Despite the wealth of new data and recent fossil discoveries, there remains several open questions about Radiodonta. Their ontogeny and development are relatively poorly known, and awaits the discovery of a wide size range of abundant species to decipher how they grew and developed. Their reproductive behavior likewise remains a mystery. Certain aspects of their morphology await clarification, for example, the precise arrangement of carapaces and sclerites in the head and their homologies with other euarthropod cephalic structures. Additionally, no consensus has yet been reached on the exact architecture of flaps and setal blades in the body trunk. Even with numerous attempts at

phylogenetic inference, the internal relationships of Radiodonta also remain largely unstable, hampering our ability to study the evolutionary dynamics of innovations such as suspension feeding, which likely evolved at least two times during the evolutionary history of these otherwise active predators. Hopefully, many of these shortcomings could be resolved in the near future with continued discoveries of new material and innovative methodological approaches. Owing to the high preservation potential of their sclerotised body parts, their highly recognisable anatomy, and their generally large size, there is a high chance of continuing to reveal exciting new Radiodonta material, which can ultimately be used to help us understand their role in early animal communities of the Cambrian Explosion.

Author contributions

The ideas have been developed in discussions between both authors. GP wrote most of the first draft of the manuscript, which was edited and expanded by AD. Photo figures were prepared by AD, and other figures were prepared by both authors. Both authors revised the article and approved the submitted version.

Funding

This research was funded by the Swiss National Science Foundation, grant number 205321_179084 entitled "Arthropod Evolution during the Ordovician Radiation: Insights from the Fezouata Biota" awarded to AD, and by the University of Lausanne.

Acknowledgments

We are grateful to the following people for providing us with images used in the figures: S. Pates, P. Cong, P. Van Roy, F. Xiao, H. Zeng, J. Paterson, J. Peel, and X. Zhang. Images by X. Zhang were sourced from the Smithsonian NMNH database, licensed under CC0. Photos of specimens taken by AD were only possible thanks to the curatorial assistance and access to specimens facilitated by S. Butts and J. Utrup at the Yale Peabody Museum (YPM); J-B. Caron, M. Akrami, D. Rudkin and P. Fenton at the Royal Ontario Museum (ROM); and M. Florence at the Smithsonian National Museum of Natural Sciences (USNM). We thank F. Pérez-Peris for advice and help us in using Gplates for the paleogeographical reconstruction. We gratefully acknowledge G. Edgecombe, G. Budd, J. Moysiuk, P. Claisse, S. Pates, P. Van Roy, and P. Gueriau for valuable discussions. We also thank P. Cong, J. Lamsdell and E. Petsios for their constructive reviews, which helped to greatly improve our manuscript.

Conflict of interest

The authors declare that the research was conducted in the absence of any commercial or financial relationships that could be construed as a potential conflict of interest.

Publisher's note

Supplementary material

The Supplementary Material for this article can be found online at: https://www.frontiersin.org/articles/10.3389/feart.2023.1160285/full#supplementary-material

References

Aria, C., and Caron, J.-B. (2015). Cephalic and limb anatomy of a new isoxyid from the Burgess Shale and the role of "stem bivalved arthropods" in the disparity of the frontalmost appendage. *PloS one* 10 (6), e0124979. doi:10.1371/journal.pone.0124979

Aria, C., Zhao, F., Zeng, H., Guo, J., and Zhu, M. (2020). Fossils from South China redefine the ancestral euarthropod body plan. *BMC Evol. Biol.* 20 (1), 4–17. doi:10.1186/s12862-019-1560-7

Bambach, R. K., Bush, A. M., and Erwin, D. H. (2007). Autecology and the filling of ecospace: Key metazoan radiations. *Palaeontology* 50 (1), 1–22. doi:10.1111/j.1475-4983.2006.00611.x

Bengtson, S. (2000). Teasing fossils out of shales with cameras and computers. *Palaeontol. Electron.* 3 (1), 14.

Bergström, J. (1986). *Opabinia* and *Anomalocaris*, unique Cambrian 'arthropods'. *Lethaia* 19 (3), 241–246. doi:10.1111/j.1502-3931.1986.tb00738.x

Bicknell, R. D. C., Ledogar, J. A., Wroe, S., Gutyler, B. C., Watson, H. W., and Paterson, J. R. (2018). Computational biomechanical analyses demonstrate similar shell-crushing abilities in modern and ancient arthropods. *Proc. Biol. Sci.* 285 (1889), 20181935. doi:10.1098/rspb.2018.1935

Bicknell, R. D. C., Schmidt, M., Rahman, I. A., Edgecombe, G. D., Gutarra, S., Daley, A. C., et al. (2023). "Raptorial appendages of the Cambrian apex predator *Anomalocaris* are built for soft prey and speed," in *Proceedings of the royal society B*. Submitted.

Bicknell, R. D. C., Smith, P. M., Howells, T. F., and Foster, J. R. (2022). New records of injured Cambrian and Ordovician trilobites. *J. Paleontology* 96, 921–929. doi:10.1017/jpa.2022.14

Boxshall, G. (2013). "Arthropod limbs and their development," in *Arthropod biology and evolution: Molecules* (Berlin, Heidelberg: Springer), 241–267.

Braddy, S. J. (2001). Eurypterid palaeoecology: Palaeobiological, ichnological and comparative evidence for a 'mass–moult–mate'hypothesis. *Palaeogeogr. Palaeoclimatol. Palaeoecol.* 172 (1-2), 115–132. doi:10.1016/s0031-0182(01)00274-7

Briggs, D. E. G. (1979). *Anomalocaris*, the largest known Cambrian arthropod. *Palaeontology* 22 (3), 631–664.

Briggs, D. E. G., and Mount, J. D. (1982). The occurrence of the giant arthropod *Anomalocaris* in the Lower Cambrian of southern California, and the overall distribution of the genus. *J. Paleontology* 56, 1112–1118.

Briggs, D. E. G., and Robison, R. A. (1984). Exceptionally preserved nontrilobite arthropods and *Anomalocaris* from the middle cambrian of Utah. *Univ. Kans. Paleontological Contributions* 111, 1–24.

Budd, G. E. (2000). "18. Ecology of nontrilobite arthropods and lobopods in the cambrian," in *The ecology of the Cambrian radiation*. Editors N. Y. C. Andrey Zhuravlev and R. Riding (West Sussex: Columbia University Press), 404–427.

Budd, G. E. (2002). A palaeontological solution to the arthropod head problem. *Nature* 417 (6886), 271–275. doi:10.1038/417271a

Budd, G. E., and Daley, A. C. (2011). The lobes and lobopods of *Opabinia regalis* from the middle Cambrian Burgess Shale. *Lethaia* 45 (1), 83–95. doi:10.1111/j.1502-3931.2011.00264.x

Budd, G. E. (1998a). The morphology and phylogenetic significance of *Kerygmachela kierkegaardi* Budd (Buen Formation, Lower Cambrian, N Greenland).

Earth Environ. Sci. Trans. R. Soc. Edinb. 89 (4), 249–290. doi:10.1017/S0263593300002418

Budd, G. E. (1998b). "Stem group arthropods from the lower cambrian Sirius Passet fauna of north Greenland," in *Arthropod relationships* (Dordrecht: Springer), 125–138. doi:10.1007/978-94-011-4904-4_11

Budd, G. E. (2021). The origin and evolution of the euarthropod labrum. *Arthropod Struct. Dev.* 62, 101048. doi:10.1016/j.asd.2021.101048

Bush, A. M., and Bambach, R. K. (2011). Paleoecologic megatrends in marine metazoa. *Annu. Rev. Earth Planet. Sci.* 39, 241–269. doi:10.1146/annurev-earth-040809-152556

Butterfield, N. J. (2000). "9. Ecology and evolution of cambrian plankton," in *The ecology of the Cambrian radiation*. Editors N. Y. C. Andrey Zhuravlev and R. Riding (West Sussex: Columbia University Press), 200–216.

Butterfield, N. J. (2002). *Leanchoilia* guts and the interpretation of three-dimensional structures in Burgess Shale-type fossils. *Paleobiology* 28 (1), 155–171. doi:10.1666/0094-8373(2002)028<0155:lgatio>2.0.co;2

Caron, J.-B., Gaines, R. R., Mángano, M. G., Streng, M., and Daley, A. C. (2010). A new Burgess Shale–type assemblage from the "thin" Stephen Formation of the southern Canadian Rockies. *Geology* 38 (9), 811–814. doi:10.1130/G31080.1

Caron, J.-B., and Jackson, D. A. (2008). Paleoecology of the greater phyllopod bed community, Burgess Shale. *Palaeogeogr. Palaeoclimatol. Palaeoecol.* 258 (3), 222–256. doi:10.1016/j.palaeo.2007.05.023

Caron, J.-B., and Moysiuk, J. (2021). A giant nektobenthic radiodont from the Burgess Shale and the significance of hurdiid carapace diversity. *R. Soc. open Sci.* 8 (9), 210664. doi:10.1098/rsos.210664

Chen, J.-y., Ramsköld, L., and Zhou, G.-q. (1994). Evidence for monophyly and arthropod affinity of Cambrian giant predators. *Science* 264 (5163), 1304–1308. doi:10.1126/science.264.5163.1304

Chen, J., Waloszek, D., and Maas, A. (2004). A new 'great-appendage'arthropod from the Lower Cambrian of China and homology of chelicerate chelicerae and raptorial antero-ventral appendages. *Lethaia* 37 (1), 3–20. doi:10.1080/00241160410004764

Chlupáč, I., and Kordule, V. (2002). Arthropods of burgess shale type from the middle cambrian of bohemia (Czech republic). *Bull. Czech Geol. Surv.* 77 (3), 167–182.

Collins, D. (1996). The "evolution" of *Anomalocaris* and its classification in the arthropod class Dinocarida (nov.) and order Radiodonta (nov.). *J. Paleontology* 70 (2), 280–293. doi:10.1017/S0022336000023362

Cong, P., Daley, A. C., Edgecombe, G. D., Hou, X., and Chen, A. (2016). Morphology of the radiodontan *Lyrarapax* from the early cambrian Chengjiang biota. *J. Paleontology* 90 (4), 663–671. doi:10.1017/jpa.2016.67

Cong, P., Daley, A. C., Edgecombe, G. D., and Hou, X. (2017). The functional head of the Cambrian radiodontan (stem-group Euarthropoda) *Amplectobelua symbrachiata*. *BMC Evol. Biol.* 17 (1), 208–223. doi:10.1186/s12862-017-1049-1

Cong, P., Ma, X., Hou, X., Edgecombe, G. D., and Strausfeld, N. J. (2014). Brain structure resolves the segmental affinity of anomalocaridid appendages. *Nature* 513 (7519), 538–542. doi:10.1038/nature13486

Cong, P. Y., Edgecombe, G. D., Daley, A. C., Guo, J., Pates, S., and Hou, X. G. (2018). New radiodonts with gnathobase-like structures from the Cambrian Chengjiang biota and implications for the systematics of Radiodonta. *Pap. Palaeontol.* 4 (4), 605–621. doi:10.1002/spp2.1219

Conway Morris, S. (1985). Cambrian lagerstätten: Their distribution and significance. *Philosophical Trans. R. Soc. Lond. B* 311, 49–65.

Daley, A. C., Antcliffe, J. B., Drage, H. B., and Pates, S. (2018). Early fossil record of Euarthropoda and the Cambrian explosion. *Proc. Natl. Acad. Sci.* 115 (21), 5323–5331. doi:10.1073/pnas.1719962115

Daley, A. C., and Bergström, J. (2012). The oral cone of *Anomalocaris* is not a classic "peytoia". *Naturwissenschaften* 99 (6), 501–504. doi:10.1007/s00114-012-0910-8

Daley, A. C., Budd, G. E., Caron, J.-B., Edgecombe, G. D., and Collins, D. (2009). The Burgess Shale anomalocaridid *Hurdia* and its significance for early euarthropod evolution. *Science* 323 (5921), 1597–1600. doi:10.1126/science.1169514

Daley, A. C., Budd, G. E., and Caron, J.-B. (2013a). Morphology and systematics of the anomalocaridid arthropod *Hurdia* from the middle cambrian of British columbia and Utah. *J. Syst. Palaeontol.* 11 (7), 743–787. doi:10.1080/14772019.2012.732723

Daley, A. C., and Budd, G. E. (2010). New anomalocaridid appendages from the Burgess Shale, Canada. *Palaeontology* 53 (4), 721–738. doi:10.1111/j.1475-4983.2010.00955.x

Daley, A. C., and Drage, H. B. (2016). The fossil record of ecdysis, and trends in the moulting behaviour of trilobites. *Arthropod Struct. Dev.* 45 (2), 71–96. doi:10.1016/j.asd.2015.09.004

Daley, A. C., and Edgecombe, G. D. (2014). Morphology of *Anomalocaris canadensis* from the Burgess Shale. *J. Paleontology* 88 (1), 68–91. doi:10.1666/13-067

Daley, A. C., and Legg, D. A. (2015). A morphological and taxonomic appraisal of the oldest anomalocaridid from the lower Cambrian of Poland. *Geol. Mag.* 152 (5), 949–955. doi:10.1017/S0016756815000412

Daley, A. C., Paterson, J. R., Edgecombe, G. D., García-Bellido, D. C., and Jago, J. B. (2013b). New anatomical information on *Anomalocaris* from the Cambrian Emu Bay Shale of South Australia and a reassessment of its inferred predatory habits. *Palaeontology* 56 (5), 971–990. doi:10.1111/pala.12029

Daley, A. C., and Peel, J. S. (2010). A possible anomalocaridid from the Cambrian Sirius Passet lagerstätte, north Greenland. *J. Paleontology* 84 (2), 352–355. doi:10.1666/09-136R1.1

De Vivo, G., Lautenschlager, S., and Vinther, J. (2021). Three-dimensional modelling, disparity and ecology of the first Cambrian apex predators. *Proc. R. Soc. B* 288, 20211176. doi:10.1098/rspb.2021.1176

Dewel, R. A., and Dewel, W. C. (1998). "The place of tardigrades in arthropod evolution," in *Arthropod relationships* (Dordrecht: Springer), 109–123. doi:10.1007/978-94-011-4904-4_10

Dick, D. G. (2015). An ichthyosaur carcass-fall community from the Posidonia Shale (Toarcian) of Germany. *Palaios* 30 (5), 353–361. doi:10.2110/palo.2014.095

Drage, H. B., and Daley, A. C. (2016). Recognising moulting behaviour in trilobites by examining morphology, development and preservation: Comment on Błażejowski et al. 2015. *BioEssays* 38 (10), 981–990. doi:10.1002/bies.201600027

Drage, H. B., Holmes, J. D., García-Bellido, D. C., and Daley, A. C. (2018a). An exceptional record of Cambrian trilobite moulting behaviour preserved in the Emu Bay Shale, South Australia. *Lethaia* 51 (4), 473–492. doi:10.1111/let.12266

Drage, H. B., Laibl, L., and Budil, P. (2018b). Postembryonic development of Dalmanitina, and the evolution of facial suture fusion in Phacopina. *Paleobiology* 44 (4), 638–659. doi:10.1017/pab.2018.31

Drage, H. B. (2019). Quantifying intra-and interspecific variability in trilobite moulting behaviour across the Palaeozoic. *Palaeontol. Electron.* 22 (2), 1–39. doi:10.26879/940

Drage, H. B., Vandenbroucke, T. R. A., Van Roy, P., and Daley, A. C. (2019). Sequence of post-moult exoskeleton hardening preserved in a trilobite mass moult assemblage from the Lower Ordovician Fezouata Konservat-Lagerstatte, Morocco. *Acta Palaeontol. Pol.* 64 (2), 261–273. doi:10.4202/app.00582.2018

Drage, H. B. (2022). Trilobite moulting behaviour variability had little association with morphometry. *bioRxiv*. 2012.520015. doi:10.1101/2022.12.12.520015

Du, K.-s., Ortega-Hernández, J., Yang, J., Yang, X.-y., Guo, Q.-h., Li, W., et al. (2020). A new early cambrian konservat-lagerstätte expands the occurrence of burgess shale-type deposits on the yangtze platform. *Earth-Science Rev.* 211, 103409. doi:10.1016/j.earscirev.2020.103409

Dunne, J. A., Williams, R. J., Martinez, N. D., Wood, R. A., and Erwin, D. H. (2008). Compilation and network analyses of Cambrian food webs. *PLoS Biol.* 6 (4), e102. doi:10.1371/journal.pbio.0060102

Edgecombe, G. D. (2020). Arthropod origins: Integrating paleontological and molecular evidence. *Annu. Rev. Ecol. Evol. Syst.* 51, 1–25. doi:10.1146/annurev-ecolsys-011720-124437

Edgecombe, G. D. (2015). Palaeontology: In a flap about flaps. *Curr. Biol.* 25 (12), R503–R506. doi:10.1016/j.cub.2015.04.029

Elzinga, R. J. (1998). Microspines in the alimentary canal of Arthropoda, Onychophora, Annelida. *Int. J. Insect Morphol. Embryology* 27 (4), 341–349. doi:10.1016/s0020-7322(98)00027-0

Estes, J. A., Terborgh, J., Brashares, J. S., Power, M. E., Berger, J., Bond, W. J., et al. (2011). Trophic downgrading of planet Earth. *science* 333 (6040), 301–306. doi:10.1126/science.1205106

Fretwell, S. D. (1987). Food chain dynamics: The central theory of ecology? *Oikos* 50, 291–301. doi:10.2307/3565489

Friedman, M., Shimada, K., Martin, L. D., Everhart, M. J., Liston, J., Maltese, A., et al. (2010). 100-million-year dynasty of giant planktivorous bony fishes in the Mesozoic seas. *Science* 327 (5968), 990–993. doi:10.1126/science.1184743

Fu, D., Legg, D. A., Daley, A. C., Budd, G. E., Wu, Y., and Zhang, X. (2022). The evolution of biramous appendages revealed by a carapace-bearing Cambrian arthropod. *Philosophical Trans. R. Soc. B* 377 (1847), 20210034. doi:10.1098/rstb.2021.0034

Guo, J., Pates, S., Cong, P., Daley, A. C., Edgecombe, G. D., Chen, T., et al. (2019). A new radiodont (stem Euarthropoda) frontal appendage with a mosaic of characters from the Cambrian (Series 2 Stage 3) Chengjiang biota. *Pap. Palaeontol.* 5 (1), 99–110. doi:10.1002/spp2.1231

Hairston, N. G., Smith, F. E., and Slobodkin, L. B. (1960). Community structure, population control, and competition. *Am. Nat.* 94 (879), 421–425. doi:10.1086/282146

Harper, D. A. T., Topper, T. P., Cascales-Miñana, B., Servais, T., Zhang, Y.-D., and Ahlberg, P. (2019). The Furogian (late Cambrian) biodiversity gap: Real or apparent? *Palaeoworld* 28 (1-2), 4–12. doi:10.1016/j.palwor.2019.01.007

Haug, J. T., Waloszek, D., Maas, A., Liu, Y., and Haug, C. (2012). Functional morphology, ontogeny and evolution of mantis shrimp-like predators in the Cambrian. *Palaeontology* 55 (2), 369–399. doi:10.1111/j.1475-4983.2011.01124.x

Holmes, J. D., García-Bellido, D. C., and Lee, M. S. Y. (2018). Comparisons between Cambrian Lagerstätten assemblages using multivariate, parsimony and Bayesian methods. *Gondwana Res.* 55, 30–41. doi:10.1016/j.gr.2017.10.007

Hou, X., Bergström, J., and Jie, Y. (2006). Distinguishing anomalocaridids from arthropods and priapulids. *Geol. J.* 41 (3-4), 259–269. doi:10.1002/gj.1050

Hou, X. G., Bergström, J., and Ahlberg, P. (1995). *Anomalocaris* and other large animals in the Lower Cambrian Chengjiang fauna of southwest China. *Gff* 117 (3), 163–183. doi:10.1080/11035899509546213

Jiao, D.-G., Pates, S., Lerosey-Aubril, R., Ortega-Hernández, J., Yang, J., Lan, T., et al. (2021). The endemic radiodonts of the cambrian stage 4 guanshan biota of South China. *Acta Palaeontol. Pol.* 66 (2), 255–274. doi:10.4202/app.00870.2020

Klug, C., Frey, L., Pohle, A., De Baets, K., and Korn, D. (2017). Palaeozoic evolution of animal mouthparts. *Bull. Geosciences* 92 (4), 511–524. doi:10.3140/bull.geosci.1648

Klug, C., Kröger, B., Kiessling, W., Mullins, G. L., Servais, T., Frýda, J., et al. (2010). The Devonian nekton revolution. *Lethaia* 43 (4), 465–477. doi:10.1111/j.1502-3931.2009.00206.x

Kühl, G., Briggs, D. E. G., and Rust, J. (2009). A great-appendage arthropod with a radial mouth from the Lower Devonian Hunsrück Slate, Germany. *Science* 323 (5915), 771–773. doi:10.1126/science.1166586

Lefebvre, B., Lerosey-Aubril, R., Servais, T., and Van Roy, P. (2016). The Fezouata Biota: An exceptional window on the Cambro-Ordovician faunal transition. *Palaeogeogr. Palaeoclimatol. Palaeoecol.* 460, 1–6. doi:10.1016/j.palaeo.2016.06.041

Legg, D. (2013). Multi-segmented arthropods from the middle Cambrian of British Columbia (Canada). *J. Paleontology* 87 (3), 493–501. doi:10.1666/12-112.1

Lendzion, K. (1975). Fauna of the mobergella zone in the polish lower Cambrian. *Geol. Q.* 19 (2), 237–242.

Lerosey-Aubril, R., Hegna, T. A., Babcock, L. E., Bonino, E., and Kier, C. (2014). Arthropod appendages from the Weeks Formation konservat-lagerstätte: New occurrences of anomalocaridids in the Cambrian of Utah, USA. *Bull. Geosciences* 89 (2), 269–282. doi:10.3140/bull.geosci.1442

Lerosey-Aubril, R., and Pates, S. (2018). New suspension-feeding radiodont suggests evolution of microplanktivory in Cambrian macronekton. *Nat. Commun.* 9 (1), 3774. doi:10.1038/s41467-018-06229-7

Lerosey-Aubril, R., Kimmig, J., Pates, S., Skabelund, J., Weug, A., and Ortega-Hernández, J. (2020). New exceptionally preserved panarthropods from the Drumian Wheeler konservat-lagerstätte of the House Range of Utah. *Pap. Palaeontol.* 6 (4), 501–531. doi:10.1002/spp2.1307

Liu, J., Lerosey-Aubril, R., Steiner, M., Dunlop, J. A., Shu, D., and Paterson, J. R. (2018). Origin of raptorial feeding in juvenile euarthropods revealed by a Cambrian radiodontan. *Natl. Sci. Rev.* 5 (6), 863–869. doi:10.1093/nsr/nwy057

Liu, Q. (2013). The first discovery of anomalocaridid appendages from the Balang Formation (Cambrian Series 2) in hunan, China. *Alcheringa Australas. J. Palaeontol.* 37 (3), 338–343. doi:10.1080/03115518.2013.753767

Liu, Y., Lerosey-Aubril, R., Audo, D., Zhai, D., Mai, H., and Ortega-Hernández, J. (2020). Occurrence of the eudemersal radiodont *Cambroraster* in the early Cambrian Chengjiang Lagerstätte and the diversity of hurdiid ecomorphotypes. *Geol. Mag.* 157 (7), 1200–1206. doi:10.1017/S0016756820000187

Luo, H. L., Li, Y., Hu, S. X., Fu, X. P., Hou, S. G., Liu, X. Y., et al. (2008). *Early Cambrian Malong fauna and Guanshan fauna from eastern Yunnan, China*. Kunming, China: Yunnan Science and Technology Press, 122.

Maas, A., Waloszek, D., Chen, J., Braun, A., Wang, X., and Huang, D. (2004). Phylogeny and life habits of early arthropods—Predation in the early Cambrian sea. *Prog. Nat. Sci.* 14 (2), 158–166. doi:10.1080/10020070412331343301

Mángano, M. G., Bromley, R. G., Harper, D. A. T., Nielsen, A. T., Smith, M. P., and Vinther, J. (2012). Nonbiomineralized carapaces in Cambrian seafloor landscapes (Sirius Passet, Greenland): Opening a new window into early Phanerozoic benthic ecology. *Geology* 40 (6), 519–522. doi:10.1130/G32853.1

Mángano, M. G., Hawkes, C. D., and Caron, J.-B. (2019). Trace fossils associated with Burgess Shale non-biomineralized carapaces: Bringing taphonomic and ecological controls into focus. *R. Soc. Open Sci.* 6 (1), 172074. doi:10.1098/rsos.172074

Mángano, M. G. (2011). Trace-fossil assemblages in a Burgess Shale-type deposit from the Stephen Formation at Stanley Glacier, Canadian Rocky Mountains: Unraveling ecologic and evolutionary controls. *Palaeontogr. Can.* 31, 89–107.

Marshall, C. R. (2006). Explaining the Cambrian "explosion" of animals. *Annu. Rev. Earth Planet. Sci.* 34, 355–384. doi:10.1146/annurev.earth.33.031504.103001

Marx, F. G., and Uhen, M. D. (2010). Climate, critters, and cetaceans: Cenozoic drivers of the evolution of modern whales. *Science* 327 (5968), 993–996. doi:10.1126/science.1185581

Mayer, G., Martin, C., de Sena Oliveira, I., Franke, F. A., and Gross, V. (2014). Latest anomalocaridid affinities challenged. *Nature* 516 (7530), E1–E2. doi:10.1038/nature13860

Mikuláš, R., Fatka, O., and Szabad, M. (2012). Paleoecologic implications of ichnofossils associated with slightly skeletonized body fossils, middle Cambrian of the Barrandian area, Czech Republic. *Ichnos* 19 (4), 199–210. doi:10.1080/10420940.2012.703626

Mironenko, A. A. (2020). Endocerids: Suspension feeding nautiloids? *Hist. Biol.* 32 (2), 281–289. doi:10.1080/08912963.2018.1491565

Moysiuk, J., and Caron, J.-B. (2019). A new hurdiid radiodont from the Burgess Shale evinces the exploitation of Cambrian infaunal food sources. *Proc. R. Soc. B* 286, 20191079. doi:10.1098/rspb.2019.1079

Moysiuk, J., and Caron, J.-B. (2022). A three-eyed radiodont with fossilized neuroanatomy informs the origin of the arthropod head and segmentation. *Curr. Biol.* 32 (15), 3302–3316.e2. doi:10.1016/j.cub.2022.06.027

Moysiuk, J., and Caron, J.-B. (2021). Exceptional multifunctionality in the feeding apparatus of a mid-Cambrian radiodont. *Paleobiology* 47, 704–724. doi:10.1017/pab.2021.19

Nedin, C. (1999). *Anomalocaris* predation on nonmineralized and mineralized trilobites. *Geology* 27 (11), 987–990. doi:10.1130/00917613(1999)027<0987:APONAM>2.3.CO;2

Nedin, C. (1995). The Emu Bay Shale, a lower Cambrian fossil lagerstätte, Kangaroo Island, South Australia. *Memoirs Assoc. Australas. Palaeontol.* 18, 31–40.

Ortega-Hernández, J. (2015). Homology of head sclerites in Burgess Shale euarthropods. *Curr. Biol.* 25 (12), 1625–1631. doi:10.1016/j.cub.2015.04.034

Ortega-Hernández, J., Janssen, R., and Budd, G. E. (2017). Origin and evolution of the panarthropod head–a palaeobiological and developmental perspective. *Arthropod Struct. Dev.* 46 (3), 354–379. doi:10.1016/j.asd.2016.10.011

Paine, R. T. (1980). Food webs: Linkage, interaction strength and community infrastructure. *J. animal Ecol.* 49 (3), 666–685. doi:10.2307/4220

Pari, G., Briggs, D. E. G., and Gaines, R. R. (2021). The Parker Quarry lagerstätte of Vermont—The first reported Burgess Shale–type fauna rediscovered. *Geology* 49 (6), 693–697. doi:10.1130/G48422.1

Pari, G., Briggs, D. E. G., and Gaines, R. R. (2022). The soft-bodied biota of the Cambrian Series 2 Parker Quarry lagerstätte of northwestern Vermont, USA. *J. Paleontology* 96 (4), 770–790. doi:10.1017/jpa.2021.125

Paterson, J. R., Edgecombe, G. D., and García-Bellido, D. C. (2020). Disparate compound eyes of Cambrian radiodonts reveal their developmental growth mode and diverse visual ecology. *Sci. Adv.* 6 (49), eabc6721. doi:10.1126/sciadv.abc6721

Paterson, J. R., Edgecombe, G. D., and Lee, M. S. Y. (2019). Trilobite evolutionary rates constrain the duration of the Cambrian explosion. *Proc. Natl. Acad. Sci.* 116 (10), 4394–4399. doi:10.1073/pnas.1819366116

Paterson, J. R., García-Bellido, D. C., Jago, J. B., Gehling, J. G., Lee, M. S. Y., and Edgecombe, G. D. (2016). The Emu Bay Shale konservat-lagerstätte: A view of Cambrian life from east Gondwana. *J. Geol. Soc.* 173 (1), 1–11. doi:10.1144/jgs2015-083

Paterson, J. R., García-Bellido, D. C., Lee, M. S. Y., Brock, G. A., Jago, J. B., and Edgecombe, G. D. (2011). Acute vision in the giant Cambrian predator *Anomalocaris* and the origin of compound eyes. *Nature* 480 (7376), 237–240. doi:10.1038/nature10689

Pates, S., Botting, J. P., McCobb, L. M. E., and Muir, L. A. (2020). A miniature Ordovician hurdiid from Wales demonstrates the adaptability of Radiodonta. *R. Soc. open Sci.* 7 (6), 200459. doi:10.1098/rsos.200459

Pates, S., Daley, A. C., and Butterfield, N. J. (2019). First report of paired ventral endites in a hurdiid radiodont. *Zool. Lett.* 5 (1), 18. doi:10.1186/s40851-019-0132-4

Pates, S., and Daley, A. C. (2017). *Caryosyntrips*: A radiodontan from the Cambrian of Spain, USA and Canada. *Pap. Palaeontol.* 3 (3), 461–470. doi:10.1002/spp2.1084

Pates, S., Daley, A. C., Edgecombe, G. D., Cong, P., and Lieberman, B. S. (2021a). Systematics, preservation and biogeography of radiodonts from the southern Great Basin, USA, during the upper Dyeran (Cambrian Series 2, Stage 4). *Pap. Palaeontol.* 7 (1), 235–262. doi:10.1002/spp2.1277

Pates, S., Daley, A. C., and Lieberman, B. S. (2018). Hurdiid radiodontans from the middle Cambrian (Series 3) of Utah. *J. Paleontology* 92 (1), 99–113. doi:10.1017/jpa.2017.11

Pates, S., Daley, A. C., and Ortega-Hernández, J. (2017). *Aysheaia prolata* from the Wheeler Formation (Cambrian, Drumian) is a frontal appendage of the radiodontan *Stanleycaris*. *Acta Palaeontol. Pol.* 62 (3). doi:10.4202/app.00361.2017

Pates, S., and Daley, A. C. (2019). The Kinzers Formation (Pennsylvania, USA): The most diverse assemblage of Cambrian Stage 4 radiodonts. *Geol. Mag.* 156 (7), 1233–1246. doi:10.1017/S0016756818000547

Pates, S., Lerosey-Aubril, R., Daley, A. C., Kier, C., Bonino, E., and Ortega-Hernández, J. (2021b). The diverse radiodont fauna from the Marjum Formation of Utah, USA (Cambrian: Drumian). *PeerJ* 9, e10509. doi:10.7717/peerj.10509

Pates, S., Wolfe, J. M., Lerosey-Aubril, R., Daley, A. C., and Ortega-Hernández, J. (2022). New opabiniid diversifies the weirdest wonders of the euarthropod stem group. *Proc. R. Soc. B* 289, 20212093. doi:10.1098/rspb.2021.2093

Perrier, V., Williams, M., and Siveter, D. J. (2015). The fossil record and palaeoenvironmental significance of marine arthropod zooplankton. *Earth-Science Rev.* 146, 146–162. doi:10.1016/j.earscirev.2015.02.003

Pimiento, C., Cantalapiedra, J. L., Shimada, K., Field, D. J., and Smaers, J. B. (2019). Evolutionary pathways toward gigantism in sharks and rays. *Evolution* 73 (3), 588–599. doi:10.1111/evo.13680

Ponomarenko, A. G. (2010). First record of Dinocarida from Russia. *Paleontological J.* 44, 503–504. doi:10.1134/S0031030110050047

Raymond, P. E. (1935). Leanchoilia *and other mid-Cambrian Arthropoda*. Cambridge, MA: Bulletin Museum of Comparative Zoology Harvard University, 76, 230.

Resser, C. E. (1929). New lower and middle Cambrian Crustacea. *Proc. U. S. Natl. Mus.* 76, 1–18. doi:10.5479/si.00963801.76-2806.1

Robison, R. A., and Richards, B. C. (1981). Larger bivalve arthropods from the middle Cambrian of Utah. *Kans. Paleontol. Contrib.* 106, 1–28.

Saleh, F., Bath-Enright, O. G., Daley, A. C., Lefebvre, B., Pittet, B., Vite, A., et al. (2021). A novel tool to untangle the ecology and fossil preservation knot in exceptionally preserved biotas. *Earth Planet. Sci. Lett.* 569, 117061. doi:10.1016/j.epsl.2021.117061

Saleh, F., Guenser, P., Gibert, C., Balseiro, D., Serra, F., Waisfeld, B. G., et al. (2022a). Contrasting Early Ordovician assembly patterns highlight the complex initial stages of the Ordovician Radiation. *Sci. Rep.* 12 (1), 3852. doi:10.1038/s41598-022-07822-z

Saleh, F., Vaucher, R., Vidal, M., Hariri, K. E., Laibl, L., Daley, A. C., et al. (2022b). New fossil assemblages from the Early Ordovician Fezouata biota. *Sci. Rep.* 12 (1), 20773. doi:10.1038/s41598-022-25000-z

Servais, T., Perrier, V., Danelian, T., Klug, C., Martin, R., Munnecke, A., et al. (2016). The onset of the 'Ordovician Plankton Revolution'in the late Cambrian. *Palaeogeogr. Palaeoclimatol. Palaeoecol.* 458, 12–28. doi:10.1016/j.palaeo.2015.11.003

Sheppard, K. A., Rival, D. E., and Caron, J.-B. (2018). On the hydrodynamics of *Anomalocaris* tail fins. *Integr. Comp. Biol.* 58 (4), 703–711. doi:10.1093/icb/icy014

Smith, C. R., Glover, A. G., Treude, T., Higgs, N. D., and Amon, D. J. (2015). Whale-fall ecosystems: Recent insights into ecology, paleoecology, and evolution. *Annu. Rev. Mar. Sci.* 7, 571–596. doi:10.1146/annurev-marine-010213-135144

Smith, M. R., and Caron, J.-B. (2015). *Hallucigenia*'s head and the pharyngeal armature of early ecdysozoans. *Nature* 523 (7558), 75–78. doi:10.1038/nature14573

Stein, M. (2010). A new arthropod from the early Cambrian of North Greenland, with a 'great appendage'-like antennula. *Zoological J. Linn. Soc.* 158 (3), 477–500. doi:10.1111/j.1096-3642.2009.00562.x

Steiner, M., Zhu, M., Zhao, Y., and Erdtmann, B.-D. (2005). Lower Cambrian Burgess Shale-type fossil associations of South China. *Palaeogeogr. Palaeoclimatol. Palaeoecol.* 220 (1-2), 129–152. doi:10.1016/j.palaeo.2003.06.001

Strausfeld, N. J. (2012). *Arthropod brains: Evolution, functional elegance, and historical significance*. Cambridge, Massachusetts: Harvard University Press.

Strausfeld, N. J., Ma, X., Edgecombe, G. D., Fortey, R. A., Land, M. F., Liu, Y., et al. (2016). Arthropod eyes: The early Cambrian fossil record and divergent evolution of visual systems. *Arthropod Struct. Dev.* 45 (2), 152–172. doi:10.1016/j.asd.2015.07.005

Sun, Z., Zeng, H., and Zhao, F. (2020a). A new middle Cambrian radiodont from north China: Implications for morphological disparity and spatial distribution of hurdiids. *Palaeogeogr. Palaeoclimatol. Palaeoecol.* 558, 109947. doi:10.1016/j.palaeo.2020.109947

Sun, Z., Zeng, H., and Zhao, F. (2020b). Occurrence of the hurdiid radiodont *Cambroraster* in the middle Cambrian (Wuliuan) Mantou Formation of north China. *J. Paleontology* 94 (5), 881–886. doi:10.1017/jpa.2020.21

Sun, Z., Zhao, F., Zeng, H., Luo, C., Van Iten, H., and Zhu, M. (2022). The middle Cambrian Linyi lagerstätte from the North China craton: A new window on Cambrian evolutionary fauna. *Natl. Sci. Rev.* 9 (7), nwac069. doi:10.1093/nsr/nwac069

Terborgh, J., and Estes, J. A. (2010). *Trophic cascades: Predators, prey, and the changing dynamics of nature*. Washington, D.C.: Island press.

Torsvik, T. H., and Cocks, L. R. M. (2017). *Earth history and palaeogeography*. Cambridge, UK: Cambridge University Press.

Usami, Y. (2006). Theoretical study on the body form and swimming pattern of *Anomalocaris* based on hydrodynamic simulation. *J. Theor. Biol.* 238 (1), 11–17. doi:10.1016/j.jtbi.2005.05.008

Van Roy, P., and Briggs, D. E. G. (2011). A giant Ordovician anomalocaridid. *Nature* 473 (7348), 510–513. doi:10.1038/nature09920

Van Roy, P., Daley, A. C., and Briggs, D. E. G. (2015). Anomalocaridid trunk limb homology revealed by a giant filter-feeder with paired flaps. *Nature* 522 (7554), 77–80. doi:10.1038/nature14256

Van Roy, P., and Tetlie, O. E. (2006). A spinose appendage fragment of a problematic arthropod from the Early Ordovician of Morocco. *Acta Palaeontol. Pol.* 51 (2), 239–246.

Vannier, J. (2007). "Early Cambrian origin of complex marine ecosystems," in *Deep time perspectives on climate change: Marrying the signal from computer models and biological proxies*. Editors M. Williams, A. M. Haywood, F. J. Gregory, and D. N. Schmidt, 81–100.

Vannier, J., and Chen, J. (2005). Early Cambrian food chain: New evidence from fossil aggregates in the Maotianshan Shale Biota, SW China. *Palaios* 20, 3–26. doi:10.2110/palo.2003.p03-40

Vannier, J., Liu, J., Lerosey-Aubril, R., Vinther, J., and Daley, A. C. (2014). Sophisticated digestive systems in early arthropods. *Nat. Commun.* 5 (1), 3641. doi:10.1038/ncomms4641

Vidal, M. (1998). Trilobites (Asaphidae and Raphiophoridae) from the Early Ordovician of the Anti-Atlas, Morocco. *Palaeontogr. Abt. A* 251, 39–77. doi:10.1127/pala/251/1998/39

Vinn, O. (2018). Traces of predation in the Cambrian. *Hist. Biol.* 30 (8), 1043–1049. doi:10.1080/08912963.2017.1329305

Vinther, J., Stein, M., Longrich, N. R., and Harper, D. A. T. (2014). A suspension-feeding anomalocarid from the early Cambrian. *Nature* 507 (7493), 496–499. doi:10.1038/nature13010

Vrazo, M. B., and Braddy, S. J. (2011). Testing the 'mass-moult-mate' hypothesis of eurypterid palaeoecology. *Palaeogeogr. Palaeoclimatol. Palaeoecol.* 311 (1-2), 63–73. doi:10.1016/j.palaeo.2011.07.031

Walcott, C. D. (1911). Cambrian geology and Paleontology II: Middle Cambrian holothurians and medusae. *Smithson. Misc. Collect.* 57 (3), 41–69.

Walcott, C. D. (1912). Middle Cambrian Branchiopoda, Malacostraca, Trilobita, and Merostomata. *Smithsonian Misc. Collect.* 57 (6), 145–228.

Wang, Y., Huang, D., and Hu, S. (2013). New anomalocardid frontal appendages from the Guanshan biota, eastern Yunnan. *Chin. Sci. Bull.* 58 (32), 3937–3942. doi:10.1007/s11434-013-5908-x

Whalen, C. D., and Briggs, D. E. G. (2018). The Palaeozoic colonization of the water column and the rise of global nekton. *Proc. R. Soc. B Biol. Sci.* 285 (1883), 20180883. doi:10.1098/rspb.2018.0883

Whiteaves, J. F. (1892). Description of a new genus and species of phyllocarid crustacea from the middle Cambrian of Mount Stephen, B.C. *Can. Rec. Sci.* V (4), 205–208.

Whittington, H. B. (1975). The enigmatic animal *Opabinia regalis*, middle Cambrian, Burgess Shale, British Columbia. *Philosophical Trans. R. Soc. Lond. B, Biol. Sci.* 271 (910), 1–43. doi:10.1098/rstb.1975.0033

Whittington, H. B., and Briggs, D. E. G. (1985). The largest Cambrian animal, *Anomalocaris*, Burgess Shale, British-columbia. *Philosophical Trans. R. Soc. Lond. B, Biol. Sci.* 309 (1141), 569–609. doi:10.1098/rstb.1985.0096

Wills, M. A., Briggs, D. E. G., and Fortey, R. A. (1998). "Evolutionary correlates of arthropod tagmosis: Scrambled legs," in *Arthropod relationships* (Dordrecht: Springer), 57–65. doi:10.1007/978-94-011-4904-4_6

Wu, Y., Fu, D., Ma, J., Lin, W., Sun, A., and Zhang, X. (2021a). *Houcaris* gen. nov. from the early Cambrian (Stage 3) Chengjiang Lagerstätte expanded the palaeogeographical distribution of tamisiocaridids (Panarthropoda: Radiodonta). *PalZ* 95 (2), 209–221. doi:10.1007/s12542-020-00545-4

Wu, Y., Ma, J., Lin, W., Sun, A., Zhang, X., and Fu, D. (2021b). New anomalocaridids (Panarthropoda: Radiodonta) from the lower Cambrian Chengjiang lagerstätte: Biostratigraphic and paleobiogeographic implications. *Palaeogeogr. Palaeoclimatol. Palaeoecol.* 569, 110333. doi:10.1016/j.palaeo.2021.110333

Wu, Y., Pates, S., Ma, J., Lin, W., Wu, Y., Zhang, X., et al. (2022). Addressing the Chengjiang conundrum: A palaeoecological view on the rarity of hurdiid radiodonts in this most diverse early Cambrian lagerstätte. *Geosci. Front.* 13 (6), 101430. doi:10.1016/j.gsf.2022.101430

Young, F. J., and Vinther, J. (2017). Onychophoran-like myoanatomy of the Cambrian gilled lobopodian *Pambdelurion whittingtoni*. *Palaeontology* 60 (1), 27–54. doi:10.1111/pala.12269

Zeng, H., Zhao, F., Niu, K., Zhu, M., and Huang, D. (2020). An early Cambrian euarthropod with radiodont-like raptorial appendages. *Nature* 588 (7836), 101–105. doi:10.1038/s41586-020-2883-7

Zeng, H., Zhao, F., Yin, Z., and Zhu, M. (2018). A new radiodontan oral cone with a unique combination of anatomical features from the early Cambrian Guanshan Lagerstätte, eastern Yunnan, South China. *J. Paleontology* 92 (1), 40–48. doi:10.1017/jpa.2017.77

Zeng, H., Zhao, F., Yin, Z., and Zhu, M. (2017). Morphology of diverse radiodontan head sclerites from the early Cambrian Chengjiang Lagerstätte, south-west China. *J. Syst. Palaeontol.* 16 (1), 1–37. doi:10.1080/14772019.2016.1263685

Zeng, H., Zhao, F., and Zhu, M. (2022). *Innovatiocaris*, a complete radiodont from the early Cambrian Chengjiang Lagerstätte and its implications for the phylogeny of Radiodonta. *J. Geol. Soc.* 180 (1), jgs2021–2164. doi:10.1144/jgs2021-164

Zhang, M., Wu, Y., Lin, W., Ma, J., Wu, Y., and Fu, D. (2023). Amplectobeluid radiodont *Guanshancaris* gen. nov. from the lower Cambrian (Stage 4) Guanshan lagerstätte of South China: Biostratigraphic and paleobiogeographic implications. *Biology* 12 (583), 583. doi:10.3390/biology12040583

Zhang, X., Shu, D., Li, Y., and Han, J. (2001). New sites of Chengjiang fossils: Crucial windows on the Cambrian explosion. *J. Geol. Soc.* 158 (2), 211–218. doi:10.1144/jgs.158.2.211

Zhao, Y. L., Zhu, M. Y., Babcock, L. E., and Peng, J. (2011). *The Kaili biota: Marine organisms from 508 million years ago*, 249. Guiyang: Guizhou Science and Technology Press.

Zhao, Y. L., Zhu, M. Y., Babcock, L. E., Yuan, J., Parsley, R. L., Peng, J., et al. (2005). Kaili biota: A taphonomic window on diversification of metazoans from the basal middle Cambrian: Guizhou, China. *Acta Geol. Sinica-English Ed.* 79 (6), 751–765. doi:10.1111/j.1755-6724.2005.tb00928.x

Zhu, X., Lerosey-Aubril, R., and Ortega-Hernández, J. (2021). Furongian (Jiangshanian) occurrences of radiodonts in Poland and South China and the fossil record of the Hurdiidae. *PeerJ* 9, e11800. doi:10.7717/peerj.11800

Zong, R.-W. (2021). Abnormalities in early Paleozoic trilobites from central and eastern China. *Palaeoworld* 30 (3), 430–439. doi:10.1016/j.palwor.2020.07.003